Zootaxa 4205 (5): 431–453
http://www.mapress.com/j/zt/

Article

ISSN 1175-5326 (print edition)
ZOOTAXA
ISSN 1175-5334 (online edition)

http://doi.org/10.11646/zootaxa.4205.5.2
http://zoobank.org/urn:lsid:zoobank.org:pub:10CF060D-EE43-46E4-92E7-E899A38CB155

Description of three new species of the tropical Asian jumping spider genus *Onomastus* Simon, 1900 from high altitude cloud forests of Sri Lanka (Araneae: Salticidae)

SURESH P. BENJAMIN[1] & NILANI KANESHARATNAM
National Institute of Fundamental Studies, Hantana road, Kandy, Sri Lanka.
E-mail: suresh.benjamin@gmail.com; nilanik4@yahoo.com
[1]Corresponding author

Abstract

Spiders of the tropical Asian jumping spider genus *Onomastus* Simon, 1900 are small to medium-sized, delicate, translucent, commonly found inhabitants of Asian evergreen forest foliage. In this paper, three new species of the genus, *O. jamestaylori* **sp. nov.** (♂♀), *O. corbetensis* **sp. nov.** (♂♀) and *O. maskeliya* **sp. nov.** (♂♀) are described from Sri Lanka. The three new species are added to the matrix of a previous study to assess their phylogenetic position. The resulting cladistic analysis, based on 35 morphological characters from 18 taxa (13 *Onomastus* species and 5 outgroups) supports the monophyly of the genus. Additionally, a monophyletic, well-supported South Asian clade (India, Sri Lanka), which is restricted to the Sri Lanka-Western Ghats biodiversity hotspot, is recovered in most analysis. The three newly described species might be endangered due to their small population size and restricted distribution in high altitude cloud forest.

Key words: Phylogeny, endemics, synapomorphies, monophyly, parsimony, India, mountaintops

Introduction

Members of the genus *Onomastus* Simon, 1900 are translucent, long-legged, small to medium-sized jumping spiders (2.0 to 5.2 mm in total length) found on foliage of tropical evergreen forests of Asia (Benjamin 2010; Maddison 2015). They do not resemble other jumping spiders in general appearance, except for their large anterior median eyes (Maddison 2015). *Onomastus* species stalk for prey and do not build capture webs (Benjamin 2010; Prószyński & Deeleman-Reinhold 2013; Wanless 1980a).

Until very recently, *Onomastus* was classified under the subfamily Lyssomaninae (Wanless 1980b), as they share characters with lyssomanines, such as the presence of four eye rows, presence of teeth on the inner posterior margin of chelicerae, limitation of tracheal system to the abdomen and general external appearance (Benjamin 2010; Galiano 1962; Zhang 2005). However, *Onomastus* can readily be distinguished from lyssomanines by the absence of a fovea, highly complex male palpal organs (with distinctive tegular apophyses not known to occur in lyssomanines) and lack of clearly defined copulatory ducts in females. Recently, Maddison (2015) revised the classification of the family Salticidae, placing *Onomastus* in a new subfamily, Onomastinae.

Onomastus currently encompasses 12 fairly well known species, mostly from the Oriental region: four species from Sri Lanka (*O. nigricaudus* Simon, 1900, *O. pethiyagodai* Benjamin, 2010, *O. quinquenotatus* Simon, 1900, and *O. rattotensis* Benjamin, 2010), two species from India (*O. indra* Benjamin, 2010 and *O. patellaris* Simon, 1900), two species from Borneo (*O. complexipalpis* Wanless, 1980 and *O. danum* Prószyński & Deeleman-Reinhold, 2013), 1 species from Thailand and Borneo (*O. kaharian* Benjamin, 2010), 1 species from China and Thailand (*O. nigrimaculatus* Zhang & Li, 2005), 1 species from Vietnam (*O. simoni* Żabka, 1985) and 1 species from Okinawa Island, Japan (*O. kanoi* Ono, 1995) (World Spider Catalog 2016).

Benjamin (2010) revised *Onomastus* and placed 10 out of the 11 species known at that time in a Phylogenetic framework. His study corroborated the monophyly of the genus and its close affinity to *Lyssomanes* [however, see

Accepted by G. Ruiz: 31 Oct. 2016; published: 9 Dec. 2016

Maddison (2015)]. Within *Onomastus*, species were grouped into two clades named as the South Asia clade, which includes species from Sri Lanka and India, and the South-East Asian clade, which includes the remaining diversity (Benjamin 2010).

An ongoing survey of spider diversity in Sri Lanka revealed the presence of an additional three species, which are described below. Further, we investigate the phylogenetic position of the three new species using a modified version the phylogenetic data matrix of Benjamin (2010).

Material and methods

Sampling was primarily done by beating vegetation up to a height of approximately 1.5 m. Methodology and taxonomic descriptions are based on the format of Benjamin (2004, 2006 and 2010). Specimens were preserved in either 70% or 100% ethanol. Spiders were identified under an Olympus SZX7 stereomicroscope. Detailed photographs of morphological features in the male palps were taken with a Hitachi S-2460 scanning electron microscope (SEM) housed at Zoological Research Museum Alexander Koenig (ZFMK). Specimens for SEM work were prepared as described in Benjamin 2004 and 2010. Female genitalia were excised and digested with Sigma Pancreatin LP 1750 enzyme complex, in a solution of sodium borate (Dingerkus & Uhler 1977). Male palps and epigynes were cleared and mounted with methyl salicyclate for further examination. Drawings of male palps, epigyne and vulva were made with the aid of a drawing tube attached to an Olympus BX51 microscope. A Nikon D80 camera with a macro lens was used to take photographs of live spiders. Photographs of palps, epigynes and intact spiders were taken with Leica MC170 HD camera mounted on a Leica M205C stereomicroscope using Leica Application Suite software (Leica Microsystems Limited, Switzerland). Images were merged with Helicon Focus image stacking software (version 6, Helicon soft Ltd). Images were edited with Adobe Photoshop CC and assembled using Adobe Illustrator CS6. All measurements are in millimeters. All specimens unless otherwise stated are deposited in the National Museum of Sri Lanka.

Abbreviations used throughout the text are: AEB: anterior epigynal border; AL: abdominal length; ALE: anterior lateral eyes; AME: anterior median eyes; AT: atrium; AR: atrial rim; AW: abdominal width; C: conductor; CD: copulatory ducts; CO: copulatory opening; CY: cymbium; E: embolus; EF: epigynal fold; EG: embolic guide; EL: epigynal lip; FD: fertilization ducts; F: femur; MA: median apophysis; MAP: mesal branch of MA; Mt: metatarsus; PA: patellar apophysis; PL: prosoma length; PLE: posterior lateral eyes; PMA: prolateral branch of MA; PME: posterior median eyes; Pt: patella; PW: prosoma width; RMA: retrolateral branch of MA; RTA: retrolateral tibial apophysis; S: spermatheca; SD: sperm duct; SP: spur mesal branch of C; T: tegulum; Ta: tarsus; TA1: tegular apophysis 1; TA3: tegular apophysis 3; Tb: tibia; TL: total length; Tr: trochanter.

Institutions mentioned throughout the text are: DFC: Department of Forest Conservation; DWLC: Department of Wildlife Conservation; NMSL: National Museum of Sri Lanka; NIFS: National Institute of Fundamental Studies; SNR: Strict Nature Reserve; ZFMK: Zoological Research Museum Alexander Koenig, Bonn.

Cladistic analysis. The character matrix was built using Mesquite (version 2.72; Maddison & Maddison 2009) for 35 potentially informative morphological characters (24 binary and 11 multistate) and scored across 18 taxa. Thirteen species of *Onomastus* and five outgroup taxa from the subfamilies Asemoneinae, Lyssomaninae and Hisponinae were included. The choice of outgroup taxa is based on Benjamin (2010). Characters of *Onomastus* spp have been scored based on original specimens, whereas outgroup taxa are scored mostly based on available literature (Table 1). The eleven multistate characters were treated as non-additive (unordered or Fitch minimum mutation model; Fitch 1971) as no transformation series could be inferred. Several autapomorphic characters have been retained in our matrix (characters 3, 9, 32, 35). Although these characters are phylogenetically uninformative, they have been included as they might be useful in other studies of salticid phylogeny based on a much larger sample of taxa and characters. Parsimony analysis of the morphological data matrix was carried out using "traditional search" mode in TNT 1.1 (Goloboff *et al.* 2008). Under equal and implied weights, traditional searches were performed with the settings of 1000 random addition sequence replicates and tree bisection reconnection (tbr) swapping algorithm, saving 10 trees per replication [see Benjamin (2011) for details]. The concavity constant (K) was set to 3–10. In memory settings, "max trees" was set to 10000. Bremer and Relative Bremer indices (Bremer 1988; Bremer 1994; Goloboff *et al.* 2003) were also calculated in TNT. Ambiguous character optimizations (Farris optimization or ACCTRAN) were resolved to favor early gains of features with subsequent reversals (Farris 1970).

Winclada version 1.00.08 (Nixon 2002) was used for mapping of characters and character states onto the most preferred parsimonious and strict consensus trees.

Systematics

Onomastus Simon, 1900

Type species: *Onomastus nigricauda* by original designation.

Onomastus jamestaylori sp. nov.

(Figs 1A–D, 2A–D, 3A–F)

Type material. Holotype: Male (IFS_SAL 552), Sri Lanka, Central Province, Kandy District, Deltota, Loolecondera, 1480 m, 07°08'45''N, 80°41'53''E, hand collection, 23 Mar. 2010, S. Batuwita & P.M.H. Sandamali. **Paratype:** Female (IFS_SAL 553), same locality and collection data, 25 Jan. 2011, S.P. Benjamin & S. Batuwita.

Other material examined. 1 male (IFS_SAL 554), same locality and collection data, 25 Jan. 2011, S.P. Benjamin & S. Batuwita; 1 male, 3 females (IFS_SAL 555–558), same locality and collection data, 30 Jun. 2011, S.P. Benjamin.

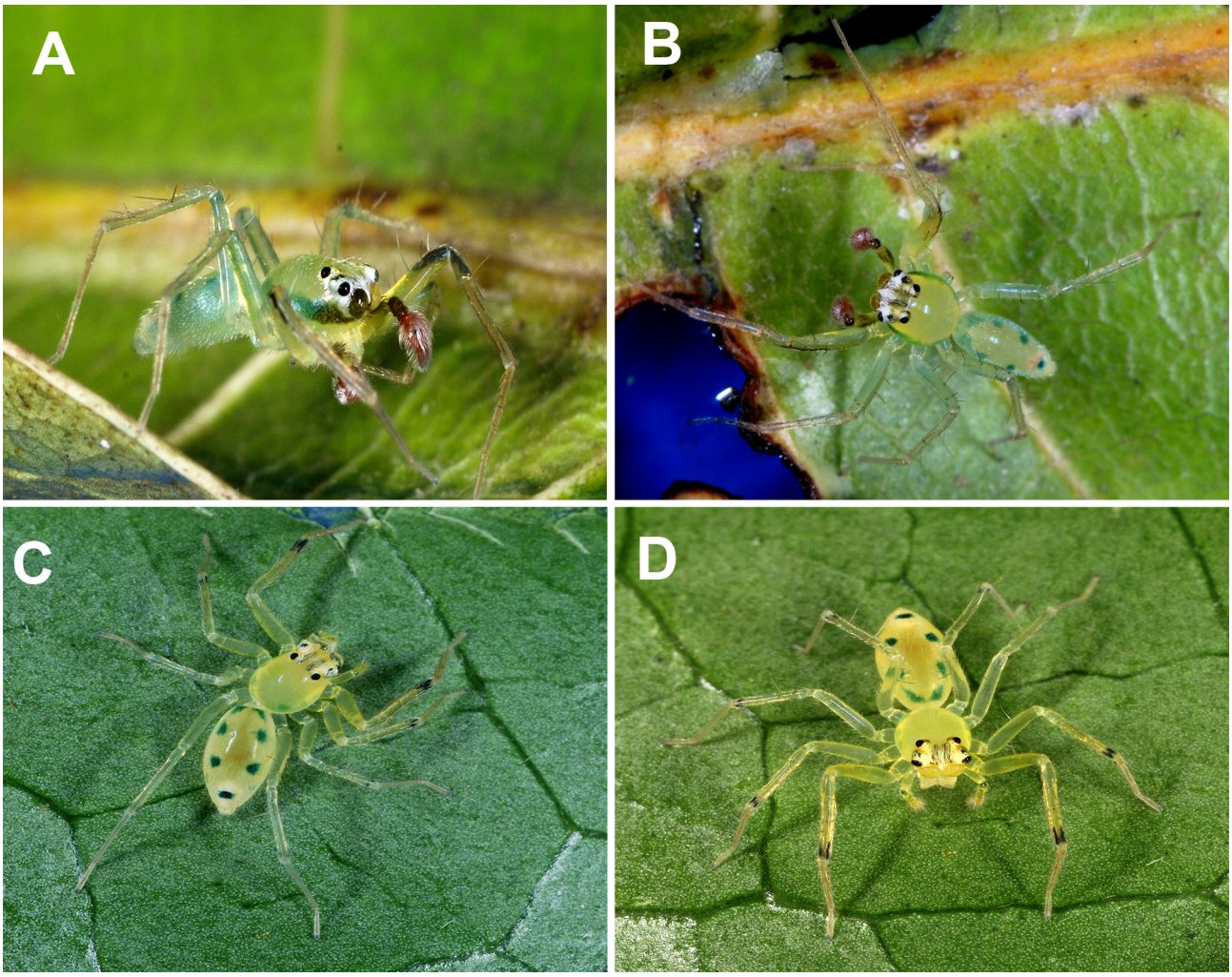

FIGURE 1. *Onomastus jamestaylori* **sp. nov.** from Loolecondera, Deltota. A–B. Male in life. C–D. Female in life.

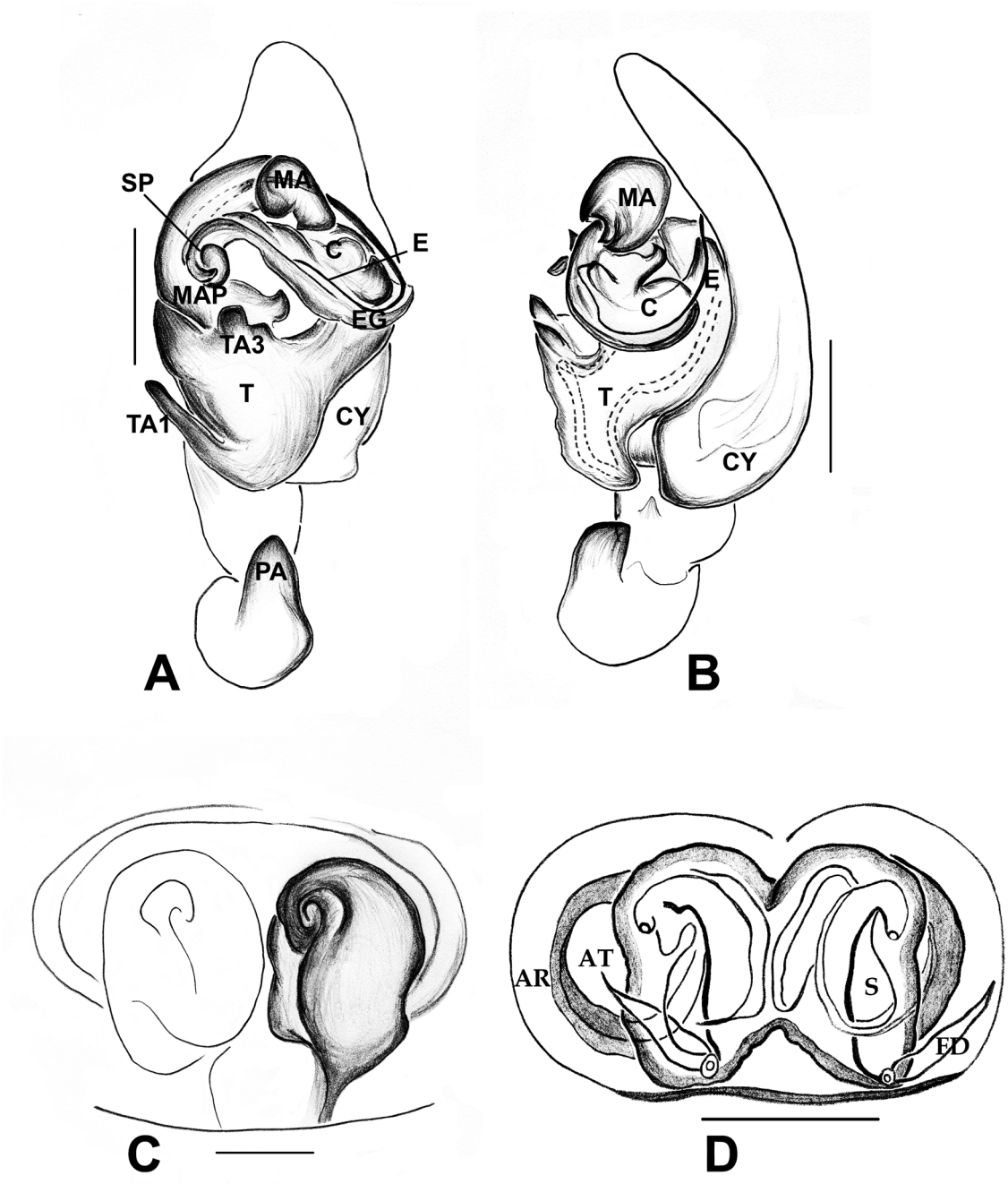

FIGURE 2. *Onomastus jamestaylori* **sp. nov.** A. Left palp, ventral view. B. Same, retrolateral view. C. Epigyne, ventral view. D. Vulva, dorsal view. Abbreviations: AR. Atrial rim; C = conductor; CY = cymbium; E = embolus; EG = embolic guide; FD = fertilization duct; MA = median apophysis; MAP = mesal branch of MA; PA = patellar apophysis; S = spermatheca; SP = spur mesal branch of conductor; T = tegulum; TA1 = tegular apophysis 1; TA3 = tegular apophysis 3. Scale bars: A–B = 0.2 mm, C–D = 0.1mm.

Etymology. This species is named after James Taylor (1835–1892), who introduced large scale tea cultivation to Sri Lanka. This species is restricted to a small forest patch in a section of his former estate.

Diagnosis. Males are distinguished by the shape of MA: broad, weakly bifurcated tip, oval spur with flaps (Figs 2A, 3A, C, D). Females are distinguished by the external appearance of the epigyne: large, broad, atrial rim present, large bean-shaped spermathecae (Figs 2C–D). This species is closely related to *O. nigricaudus* by the presence of partially bifurcated distal end of MA. However, it differs by the presence of equal sized prolateral and retrolateral arms of MA in males and absence of atrial rim, shape of spermathecae and absence of inverted u-shaped epigynal bars in females.

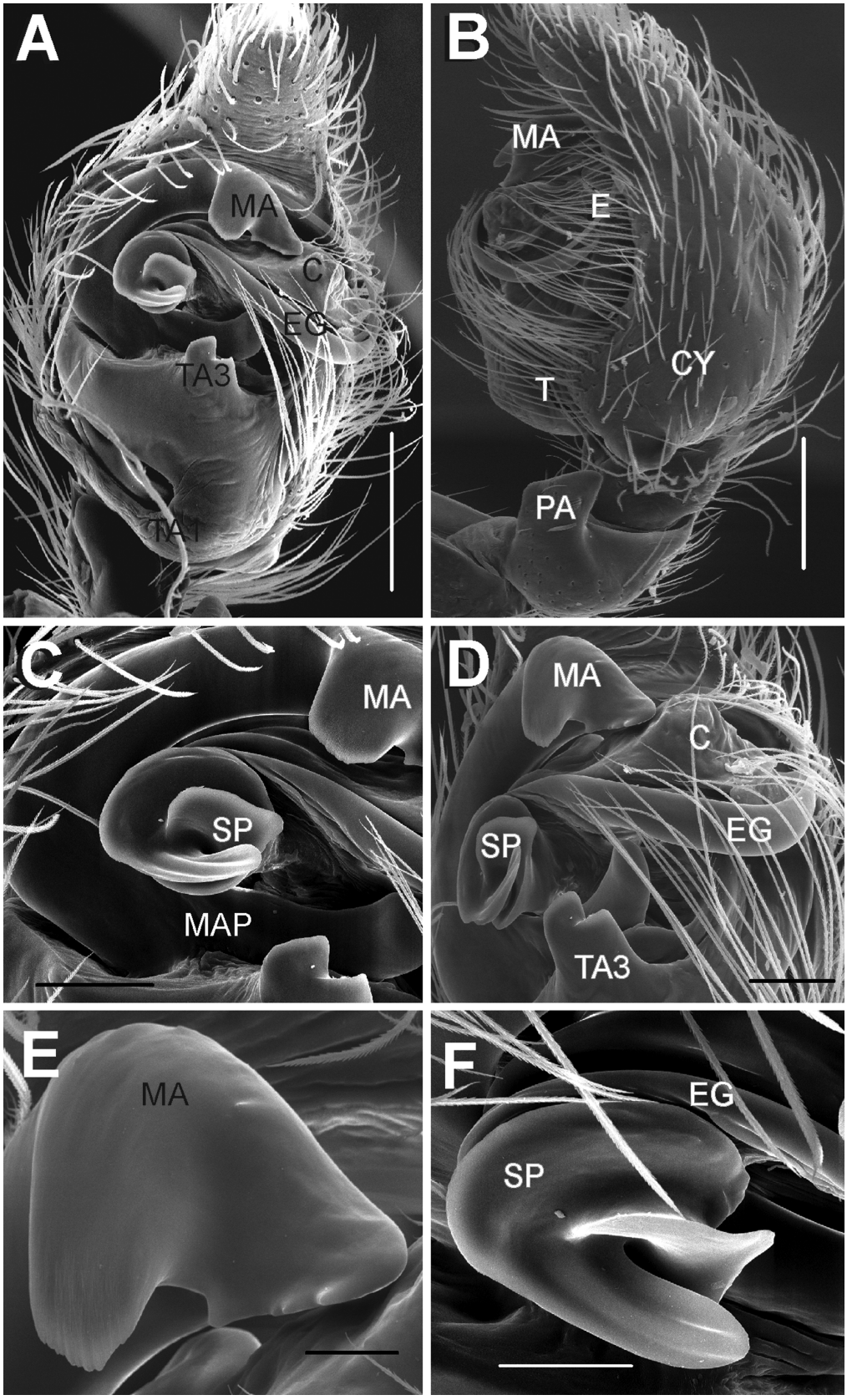

FIGURE 3. Scanning electron micrographs of *Onomastus jamestaylori* **sp. nov.** A, C, D. Left male palp, ventral view. B. Same, retrolateral view. E. Distal end of MA, ventral view. F. Mesal spur, ventral view. Abbreviations: C = conductor; CY = cymbium; E = embolus; EG = embolic guide; MA = median apophysis; MAP = mesal branch of MA; PA = patellar apophysis; SP = spur mesal branch of C; T = tegulum; TA1 = tegular apophysis 1; TA3 = tegular apophysis 3. Scale bars: A–B = 200 µm, C = 60 µm, D = 80 µm, E = 30 µm, F = 40 µm.

Description. Male holotype: yellowish green in life (Figs 1A–B). Lateral sides of prosoma bordered in dark green (Figs 1A–B). Specimens preserved in ethanol, light yellow. Chelicerae yellowish green with 3 promarginal and 7 retromarginal teeth. Labium yellowish green, as wide as long. Scutiform sternum with vague margins. Ocular region densely clothed with glossy white hairs (Figs 1A–B). All eyes black, except for the greenish yellow anterior medians, placed on low, black tubercles. Eye field broader anteriorly than posteriorly, occupying nearly half of the prosoma. PMEs much smaller, positioned on black tubercles. Median ocular quadrangle wider than long. Prosoma moderately high, rounded, slightly longer than wide. Posterior prosoma slopes gradually, rounded, without any truncation. Abdomen: oval, longer and narrower than prosoma, tapering toward posterior end. Dorsum yellowish green with pairs of dark green spots on the lateral sides (Figs 1A–B). Venter yellowish green without any markings. Spinnerets yellowish green. Legs: front legs greenish brown, somewhat darker than others, femur I and patella I with dark black markings (Fig. 1A), other legs yellowish green. Male palp: greenish brown with reddish brown palpal tibia; cymbium and bulbus large. Cymbium with distal finger-like extension. Highly sclerotized median apophysis, curved to a semi-circular arch, ending in broad, weakly bifurcated terminal structure with serrated tips (Figs 2A–B, Figs 3A–E). Retrolateral patellar apophysis broad, tip blunt (Figs 2A–B, 3B). Embolus originates from alveolar cavity, moderately long, thread-like. Conductor tapering (Figs 2A–B, 3A, B, D), lying between median apophysis and tegulum, with heavily sclerotized embolic guide, terminates in a broad, oval, spur, armed with two hooks (Figs 2A, 3A, C, D). Mesal branch of MA supports spur and embolic guide. TA1 long and finger-like, TA3 prominent, broad, short, clearly visible. Measurements: TL 2.85, PL 1.30, PW at PLEs 1.05, AL 1.60, AW 0.75. Eye field: Diameter of AME 0.34, PLE 0.12, ALE 0.20, PME 0.01, PME–PME 0.62, PLE–PLE 0.46, ALE–PME 0.09, ALE–PLE 0.31. Leg I: Tr 0.10, Fm 1.36, Pt 0.37, Tb 1.24, Mt 0.84, Ta 0.40; Leg II: Tr 0.10, Fm 1.24, Pt 0.31, Tb 1.24, Mt 0.96, Ta 0.37; Leg III: Tr 0.10, Fm 1.30, Pt 0.34, Tb 1.18, Mt 1.27, Ta 0.34; Leg IV: Tr 0.10, Fm 1.33, Pt 0.31, Tb 1.27, Mt 1.40, Ta 0.34.

Female paratype: As in males, except: eye field occupying nearly one third of prosoma, lateral sides of prosoma without dark green markings, abdomen broader, prominent pairs of dark green spots in the anterior, tibiae of all legs with black patches and tibia I with larger, prominent patches (Figs 1C–D). Epigyne: relatively less sclerotized. Large atrial rim present (Figs 2C–D). Copulatory openings clearly visible, situated anterolaterally to the bean-shaped spermathecae. Spermathecae appear to be fused. Fertilization ducts lanceolate, long, slender, originating from middle of postero-dorsal wall of receptacles. Measurements: TL 3.75, PL 1.75, PW at PLEs 0.95, AL 1.85, AW 0.95. Eye field: Diameter of AME 0.34, PLE 0.09, ALE 0.22, PME 0.02, PME–PME 0.59, PLE–PLE 0.47, ALE–PME 0.12, ALE–PLE 0.34. Leg I: Tr 0.12, Fm 1.24, Pt 0.40, Tb 1.18, Mt 0.76, Ta 0.43; Leg II: Tr 0.09, Fm 1.27, Pt 0.34, Tb 1.05, Mt 0.84, Ta 0.34; Leg III: Tr 0.16, Fm 1.27, Pt 0.31, Tb 1.09, Mt 0.81, Ta 0.34; Leg IV: Tr 0.12, Fm 1.36, Pt 0.34, Tb 1.27, Mt 1.36, Ta 0.56.

***Onomastus corbetensis* sp. nov.**
(Figs 4A–D, 5A–D, 6A–E)

Type material. Holotype: Male (IFS_SAL 559), Sri Lanka, Central Province, Kandy District, Corbett's Gap, Knuckles range, 1360 m, 07°21'40''N, 80°50'00''E, hand collection, 12 Aug. 2010, S.P. Benjamin & S. Batuwita. **Paratype.** Female (IFS_SAL 560), same locality and collection data, 19 Aug. 2010.

Other material examined: 1 male, 2 females (IFS_SAL 561–563), same locality and collection data, 19 Aug. 2010.

Etymology. Named after the type locality; to be treated as an adjective.

Diagnosis. Males are distinguished by the strongly forked MA with a pleated prolateral branch and a tapering, hook-shaped tip (Figs 5A, 6B, D). Females are distinguished by the shape of the epigyne, rounded spermathecae with shallow indentation in mid-lateral wall (Fig 5C–D). This species is closely related to *O. rattotensis* by the strongly bifurcated distal end of MA, pleated prolateral arm, well-developed curved retrolateral arm, shape of conductor spur and rounded spermathecae. However, it differs by the presence of a hook-shaped prolateral arm, retrolateral arm terminating in faintly serrated tip in males and broad anterior epigynal border in females.

Description. Male holotype: pale green in life; ethanol preserved specimens light yellow. Chelicerae pale green with 3 promarginal, 7 retromarginal teeth. Pale green labium, as wide as long. Scutiform sternum with vague margins. Ocular region densely covered with glossy white hairs. All eyes black, except for the greenish yellow

anterior medians, placed on low, black tubercles (Figs 4A–B). Eye field broader anteriorly than posteriorly, occupying nearly half of the prosoma. PMEs much smaller positioned on black tubercles. Median ocular quadrangle wider than long. Prosoma moderately high, rounded, slightly longer than wide. Posterior prosoma slopes gradually, rounded, without any truncation. Abdomen: elongate, ovoid, longer and narrower than prosoma, tapering toward posterior end. Dorsum pale green with dull green blotches on the lateral sides (Figs 4A–B). Venter pale green, no markings, spinnerets pale green. Legs: pale green without any markings. Male palp: pale green palp with faint brown palpal tibia, cymbium and bulbus. Cymbium with distal finger-like extension. Highly sclerotized, branched median apophysis. Pleated prolateral branch of MA with hook-shaped tip, retrolateral branch strongly curved, end in a faintly serrated tip (Figs 5A, 6B, D). Retrolateral patellar apophysis much broader tapered with rounded tip (Figs 5A–B, 6B–C). Filamentous, medium sized embolus originating from alveolar cavity. Conductor tapering (Figs 5A–B, 6B–D), lying between median apophysis and tegulum, heavily sclerotized embolic guide, terminus shape of spur with two pointed hooks (as in Figs 5A, 6B, D, E). Mesal branch of MA supports spur and embolic guide. TA1 long and finger-like, TA3 short, broad. Measurements: TL 2.80, PL 1.50, PW at PLEs 0.95, AL 1.40, AW 0.80. Eye field: Diameter of AME 0.34, PLE 0.12, ALE 0.19, PME 0.02, PME–PME 0.59, PLE–PLE 0.46, ALE–PME 0.12, ALE–PLE 0.31. Leg I: Tr 0.10, Fm 1.30, Pt 0.40, Tb 1.27, Mt 0.84, Ta 0.40; Leg II: Tr 0.12, Fm 1.27, Pt 0.37, Tb 1.24, Mt 0.99, Ta 0.34; Leg III: Tr 0.09, Fm 1.27, Pt 0.34, Tb 1.21, Mt 1.27, Ta 0.31; Leg IV: Tr 0.12, Fm 1.43, Pt 0.34, Tb 1.27, Mt 1.43, Ta 0.31.

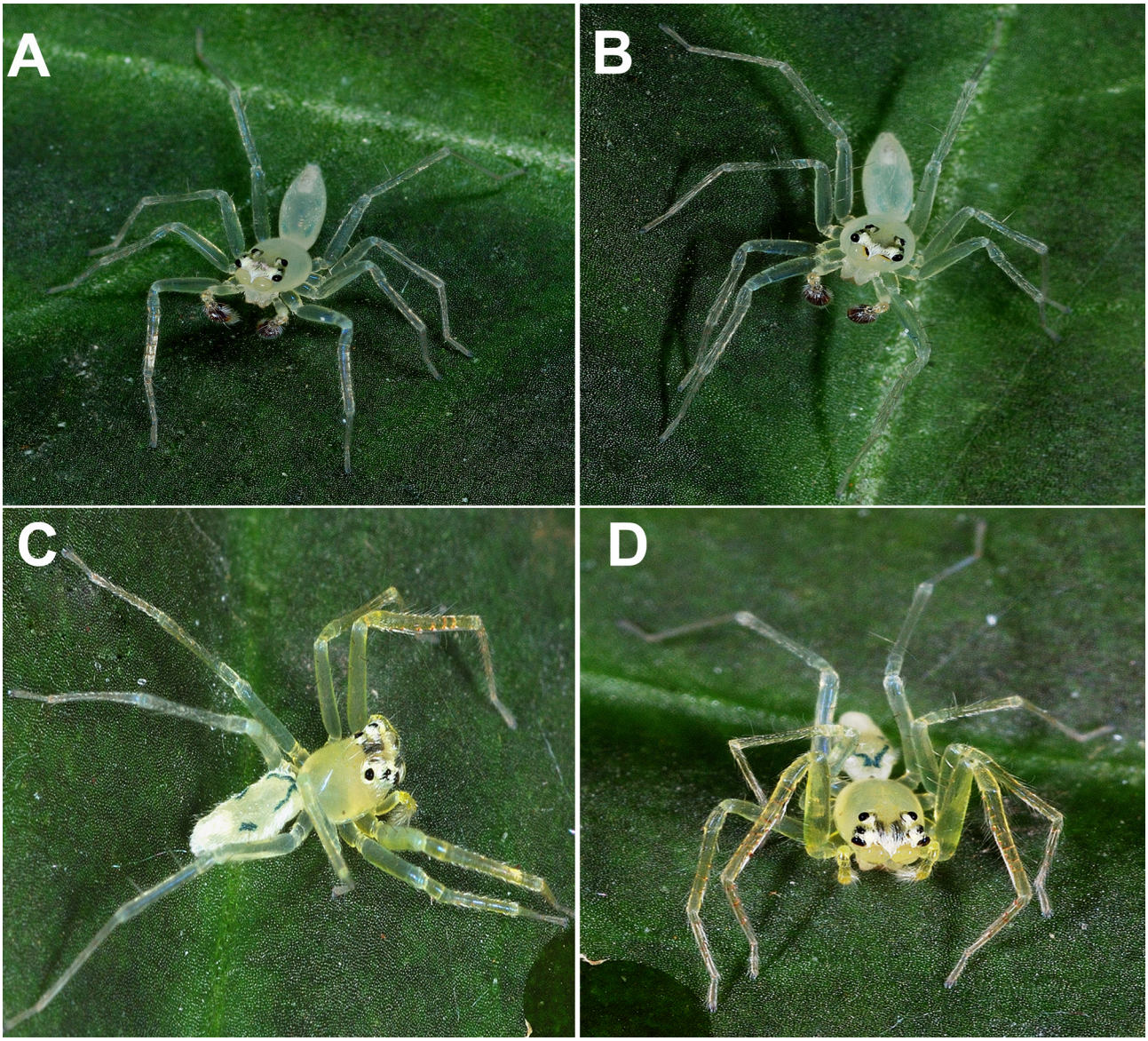

FIGURE 4. *Onomastus corbetensis* **sp. nov.** from Corbett's Gap, Knuckles range. A–B. Male in life. C–D. Female in life.

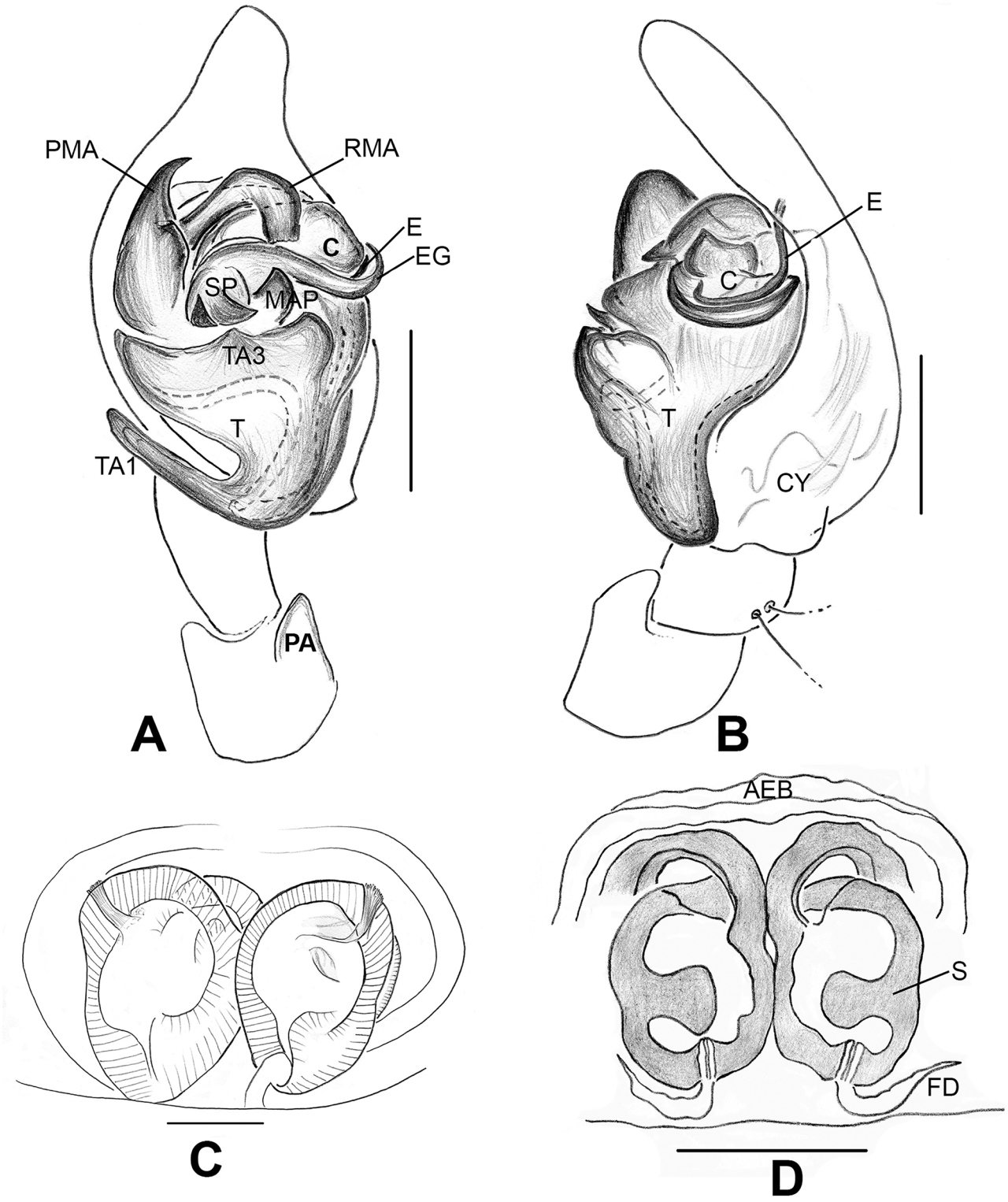

FIGURE 5. *Onomastus corbetensis* **sp. nov.** A. Left palp, ventral view. B. Same, retrolateral view. C. Epigyne, ventral view. D. Vulva, dorsal view. Abbreviations: AEB = anterior epigynal border; C = conductor; CY = cymbium; E = embolus; EG = embolic guide; FD = fertilization duct; MAP = mesal branch of MA; PA = patellar apophysis; PMA = prolateral branch of MA; RMA = retrolateral branch of MA; S = spermatheca; SP = spur mesal branch of conductor; T = tegulum; TA1 = tegular apophysis 1; TA3 = tegular apophysis 3. Scale bars: D = 0.1 mm, A–C = 0.2 mm.

Female paratype: As in male, except: yellowish green prosoma, eye field occupying nearly one third of prosoma, prominent black marking in the middle of eye field, broad abdomen with prominent dark green markings (Figs 4C–D). Epigyne: very sclerotized. Anterior epigynal border with broad, sclerotized hood-like structure.

Atrial rim present, copulatory openings directly open into spermathecae, spermathecae large, somewhat rounded, small indentation mid-laterally, sclerotized thick walls (Figs 5C–D). Fertilization ducts lanceolate, long, slender, originating from middle of postero-dorsal wall of receptacles. Measurements: TL 3.65, PL 1.35, PW at PLEs 0.90, AL 2.20, AW 1.10. Eye field: Diameter of AME 0.37, PLE 0.09, ALE 0.12, PME 0.02, PME–PME 0.62, PLE–PLE 0.67, ALE–PME 0.12, ALE–PLE 0.31. Leg I: Tr 0.16, Fm 1.55, Pt 0.43, Tb 1.21, Mt 0.81, Ta 0.40; Leg II: Tr 0.10, Fm 1.24, Pt 0.31, Tb 1.05, Mt 0.81, Ta 0.31; Leg III: Tr 0.16, Fm 1.30, Pt 0.31, Tb 1.05, Mt 0.81, Ta 0.31; Leg IV: Tr 0.12, Fm 1.33, Pt 0.34, Tb 1.27, Mt 1.33, Ta 0.53.

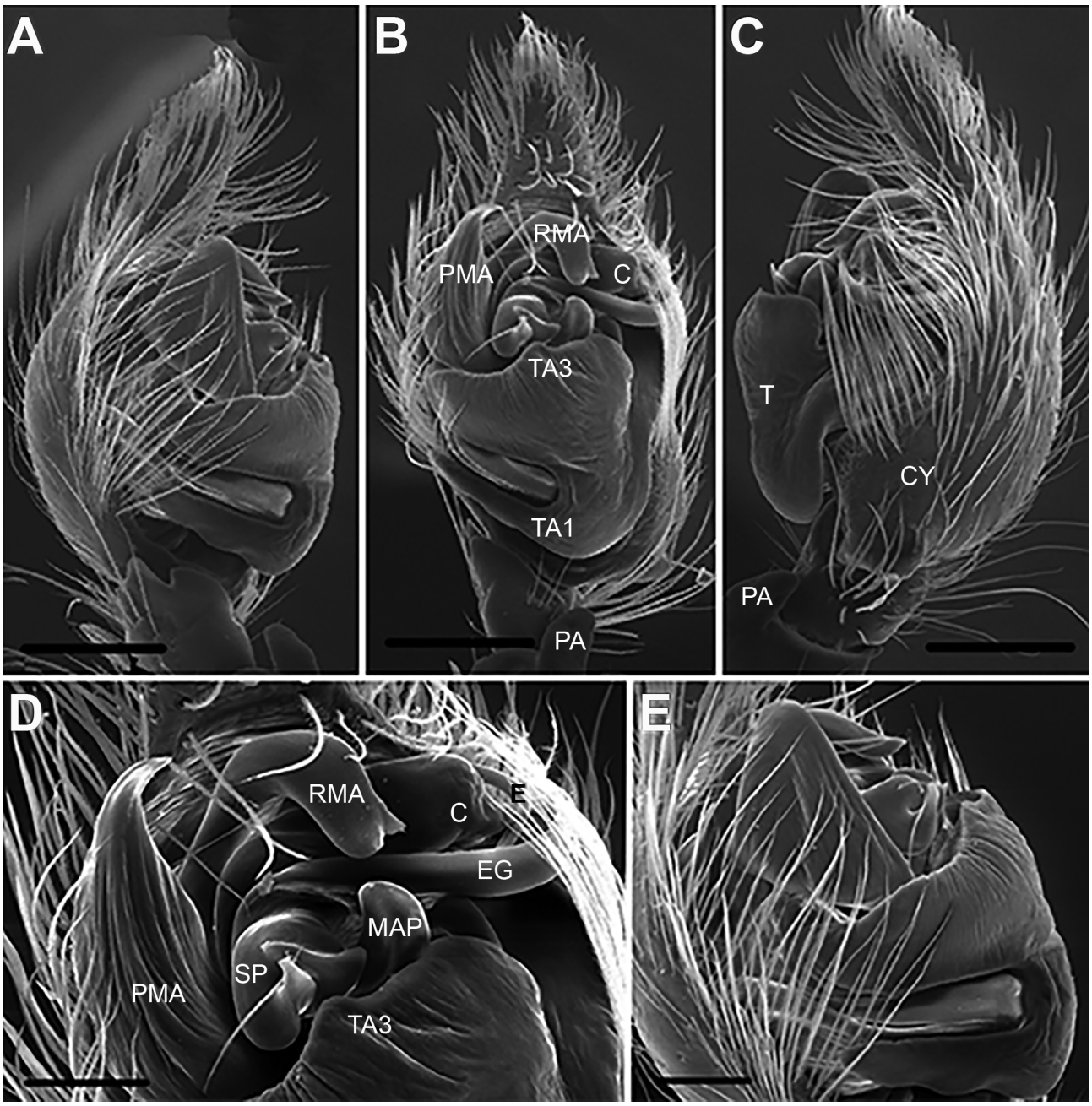

FIGURE 6. Scanning electron micrographs of *Onomastus corbetensis* **sp. nov.** A, E. Left male palp, prolateral view. B, D. Same, ventral view. C. Same, retrolateral view. Abbreviations: C = conductor; CY = cymbium; E = embolus; EG = embolic guide; MAP = mesal branch of MA; PA = patellar apophysis; PMA = prolateral branch of MA; RMA = retrolateral branch of MA; SP = spur mesal branch of C; T = tegulum; TA1 = tegular apophysis 1; TA3 = tegular apophysis 3. Scale bars: D = 80 μm, E = 100 μm, A–C = 200 μm.

***Onomastus maskeliya* sp. nov.**
(Figs. 7A–D, 8A–D, 9A–E)

Type material. Holotype: Male (IFS_SAL 564), Sri Lanka, Central Province, Nuwara Eliya District, Maskeliya, Upcott, 1850 m, 06°46'N, 80°36'E, hand collection, 2 Feb. 2011, S.P. Benjamin & S. Batuwita. **Paratype:** Female (IFS_SAL 565), same locality and collection data, 14 Feb. 2012, S.P. Benjamin & N. Athukorala.

Other material examined. 1 male, 2 females (IFS_SAL 566–568), same locality and collection data, 14 Feb. 2012, S.P. Benjamin & N. Athukorala.

Etymology. Named after the type locality; used as a noun in apposition.

Diagnosis. Males are distinguished by the unbranched MA, curved tip of MA, shape of the conductor spur (Figs 8A, 9A–E). Females are distinguished by the comparably broader epigyne, inverted pear-shaped, thick walled, highly sclerotized, spermathecae (Figs 8C–D). This species is related to *O. quinquenotatus* and *O. pethiyagodai* by the presence of a smooth and tapered MA and inverted pear-shaped spermathecae. However, it differs from both species by the globular-shaped terminus of MA, absence of prominent apical hump of MA in males and presence of atrial rim, broad AEB and large receptacles in females.

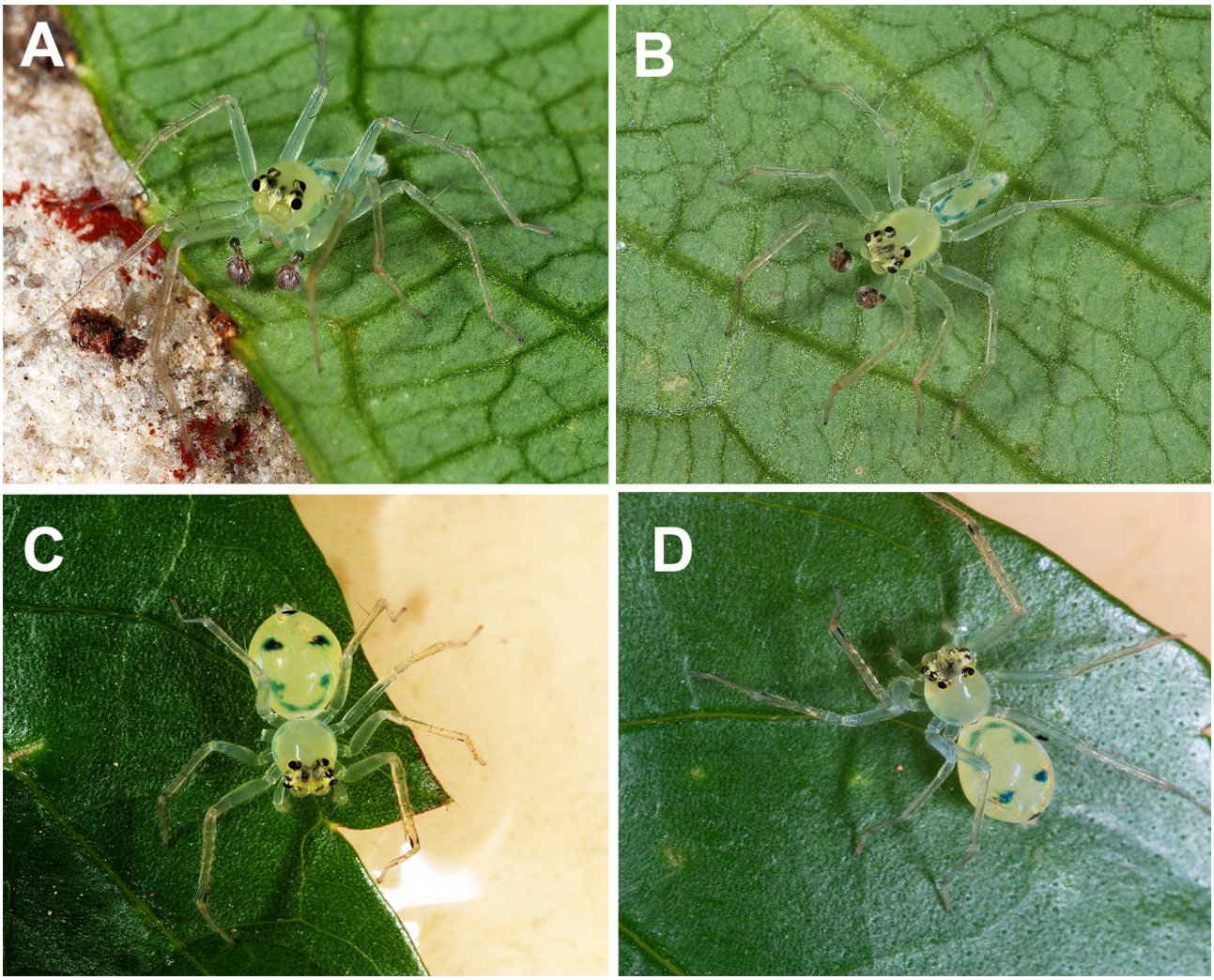

FIGURE 7. *Onomastus maskeliya* **sp. nov.** from Upcott. A–B. Male in life. C–D. Female in life.

Description. Male holotype: yellowish green carapace, pale green color laterals in live spiders (Figs 7A–B). Spiders preserved in ethanol faded yellow in color. Pale green chelicerae, fawn color tip, 3 promarginal and 7 retromarginal teeth. Labium yellowish green, wider than long. Scutiform sternum with vague margins. Ocular region sparsely clothed with white hairs. All eyes black in color, placed on low tubercles, except for greenish yellow, anterior medians. Eye field with prominent black patches in the center (Figs 7A–B), broader anteriorly than

posteriorly, occupying about half of the prosoma. PMEs much smaller, positioned on black tubercles. Median ocular quadrangle wider than long. Prosoma moderately high, rounded, longer than wide. Posterior prosoma slopes gradually rounded, without truncation. Abdomen: elongate, ovoid, longer and narrower than prosoma, tapering toward posterior end. Dorsum yellowish green, lateral with dark green characteristic pattern (Figs 7A–B). Venter yellowish green, no markings. Spinnerets yellowish green. Legs: pale green without any markings. Male palp: pale green with brown palpal tibia; cymbium and bulbus large, with distal finger-like extension. Median apophysis well sclerotized, no branches, tip rounded (Figs 8A, 9B, D, E). Retrolateral patellar apophysis broad, tip blunt (Figs 8A–B, 9A–C). Embolus originates from the alveolar cavity, moderately long, thread-like. Conductor filiform, lying between median apophysis and tegulum, with heavily sclerotized embolic guide that terminates in a comparably larger and broader hook-shape of spur (Figs 8A, 9A–E). Spur and embolic guide supported by mesal branch of MA. TA1, long, finger-like, TA3 prominent, broad short. Measurements: TL 2.85, PL 1.30, PW at PLEs 1.05, AL 1.40, AW 0.70. Eye field: Diameter of AME 0.37, PLE 0.10, ALE 0.22, PME 0.01, PME–PME 0.62, PLE–PLE 0.49, ALE–PME 0.09, ALE–PLE 0.31. Leg I: Tr 0.12, Fm 1.08, Pt 0.34, Tb 1.30, Mt 0.65, Ta 0.46; Leg II: Tr 0.12, Fm 1.15, Pt 0.31, Tb 1.27, Mt 0.77, Ta 0.40; Leg III: Tr 0.12, Fm 1.21, Pt 0.37, Tb 1.18, Mt 1.33, Ta 0.56; Leg IV: Tr 0.15, Fm 1.21, Pt 0.34, Tb 1.36, Mt 0.99, Ta 0.56.

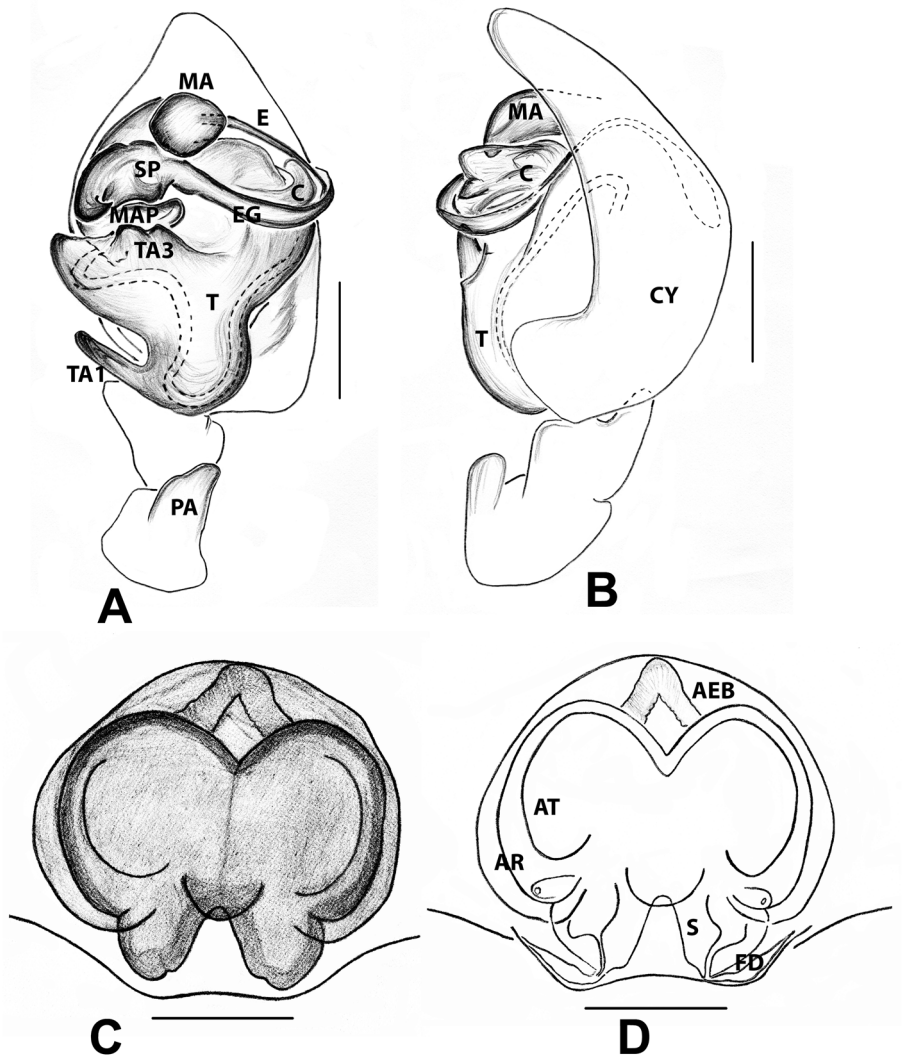

FIGURE 8. *Onomastus maskeliya* **sp. nov.** A. Left palp, ventral view. B. Same, retrolateral view. C. Epigyne, ventral view. D. Vulva, dorsal view. Abbreviations: AEB = anterior epigynal border; AR. Atrial rim; AT = atrium; C = conductor; CY = cymbium; E = embolus; EG = embolic guide; FD = fertilization duct; MA = median apophysis; MAP = mesal branch of MA; PA = patellar apophysis; S = spermatheca; SP = spur mesal branch of conductor; T = tegulum; TA1 = tegular apophysis 1; TA3 = tegular apophysis 3. Scale bars: D = 0.1 mm, A–C = 0.2 mm.

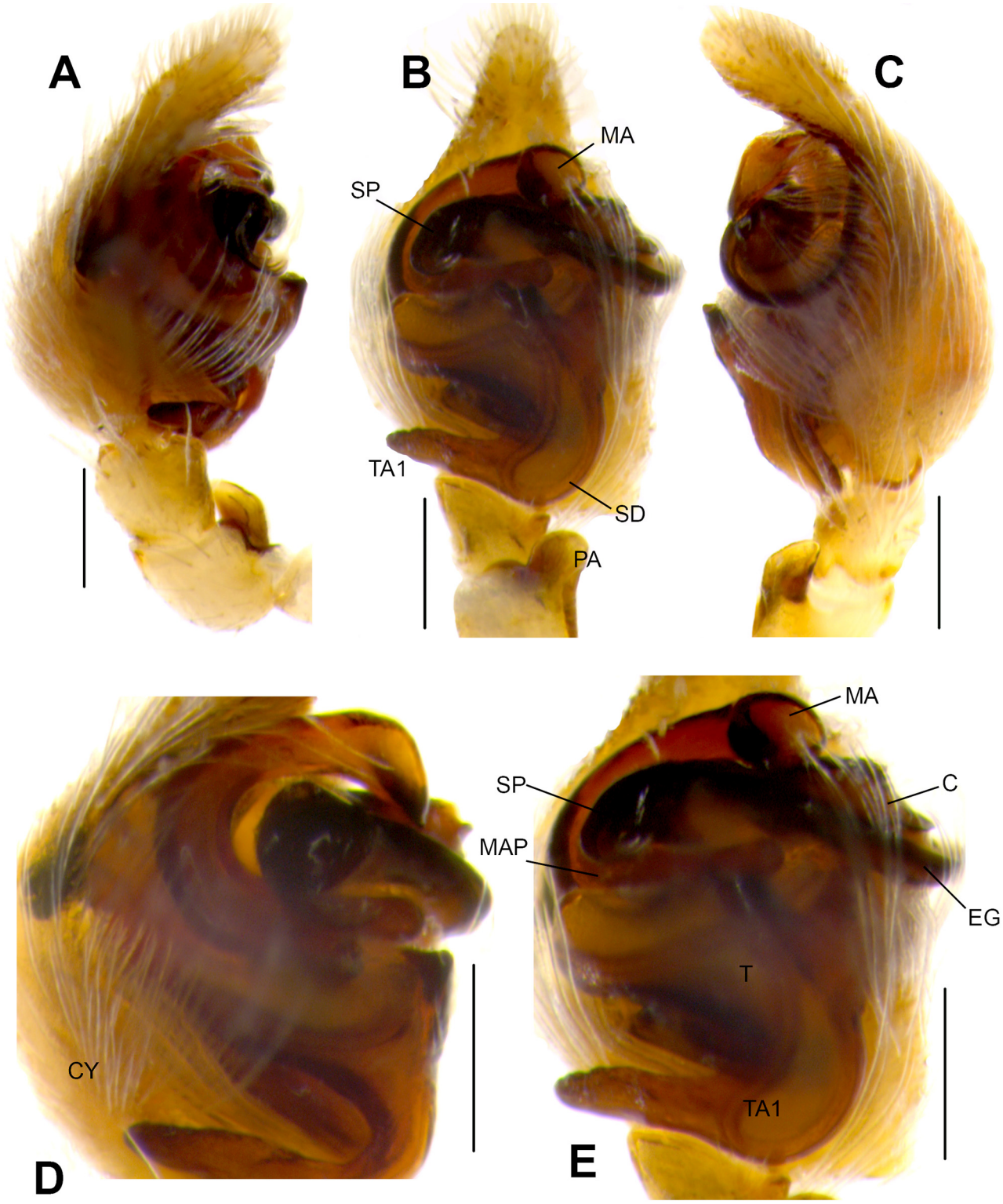

FIGURE 9. *Onomastus maskeliya* **sp. nov.** A, D. Left palp, prolateral view. B, E. Same, ventral view. C. Same, retrolateral view. Abbreviations: C = conductor; CY = cymbium; EG = embolic guide; MA = median apophysis; MAP = mesal branch of MA; PA = patellar apophysis; SD = sperm duct; SP = spur mesal branch of conductor; T = tegulum; TA1 = tegular apophysis 1. Scale bars: A–E = 0.2 mm.

Female paratype: As in male, except: yellowish green prosoma, eye field occupying nearly one third of the prosoma, abdomen yellowish, broader, with peculiar dark green blotches (Figs 7C–D). Epigyne: broad, well sclerotized. Large atrial rim present (Figs 8C–D). Copulatory openings seem to open directly into spermathecae. Spermathecae large, inverted pear-shaped, with heavily sclerotized thick wall (Figs 8C–D). Spermathecae appear

to be fused. Fertilization ducts lanceolate, moderately long, slender, originating from middle of postero-dorsal wall of receptacles (Fig. 8D). Measurements: TL 3.95, PL 1.40, PW at PLEs 0.95, AL 1.80, AW 1.40. Eye field: Diameter of AME 0.37, PLE 0.09, ALE 0.22, PME 0.02, PME–PME 0.62, PLE–PLE 0.47, ALE–PME 0.09, ALE–PLE 0.31. Leg I: Tr 0.16, Fm 1.02, Pt 0.46, Tb 1.30, Mt 1.12, Ta 0.46; Leg II: Tr 0.12, Fm 1.24, Pt 0.40, Tb 1.27, Mt 0.93, Ta 0.43; Leg III: Tr 0.16, Fm 1.12, Pt 0.34, Tb 1.24, Mt 0.87, Ta 0.40; Leg IV: Tr 0.16, Fm 1.58, Pt 0.34, Tb 1.30, Mt 1.55, Ta 0.50.

Key to adult males of Sri Lankan *Onomastus*

1. MA with pleated prolateral branch (Figs 5A, 6B; Benjamin 2010: fig. 27a) 2
- MA without pleated prolateral branch 3
2. Prolateral branch of MA, hook-shaped (Figs 5A, 6B) . . . . . ***O. corbetensis* sp. nov.**
- Prolateral branch of MA with rounded tip (Benjamin 2010: fig. 27a) . . . . . *O. rattotensis*
3. Terminus of MA bifurcated (Figs 2A, 3A) 4
- Terminus of MA not bifurcated, globular with stout or pointed tip. 5
4. Prolateral branch of MA terminus, smaller than the retrolateral branch (Benjamin 2010: fig. 10a) . . . . . *O. nigricauda*
- Prolateral and retrolateral branches of equal size (Figs 2A, 3A) . . . . . ***O. jamestaylori* sp. nov.**
5. Terminus of MA globular but without any prominent apical hump (Fig. 8A) . . . . . ***O. maskeliya* sp. nov.**
- Terminus of MA with apical hump 6
6. Terminus of MA with pointed tip (Benjamin 2010: fig. 22a) . . . . . *O. quinquenotatus*
- Terminus of MA with stout tip (Benjamin 2010: fig. 23b) . . . . . *O. pethiyagodai*

Key to adult females of Sri Lankan *Onomastus*

1. S irregular in shape, with inverted u-shaped epigynal bars (Benjamin 2010: fig. 10e) . . . . . *O. nigricauda*
- S otherwise, epigynal bars absent 2
2. S rounded. 3
- S oval. 4
3. S with shallow indentation on mid-lateral wall, broad AEB, sclerotized hood-like structure, curved atrium rim (Figs 5C, D) . . . . . ***O. corbetensis* sp. nov.**
- S without any indentation, rounded (Benjamin 2010: figs 26d, e) . . . . . *O. rattotensis*
4. S bean-shaped, large with mid-longitudinal sclerotized bars, large atrium rim (Figs 2C, D). . . . . ***O. jamestaylori* sp. nov.**
- S inverted pear-shaped 5
5. Epigyne broad, well sclerotized, with broad AEB, large atrial rim (Figs 8C, D) . . . . . ***O. maskeliya* sp. nov.**
- Epigyne narrower, without AEB 6
6. FD large and lanceolate (Benjamin 2010: figs 21b, c) . . . . . *O. pethiyagodai*
- FD small and filamentous (Benjamin 2010: figs 24c, d) . . . . . *O. quinquenotatus*

Description of characters and character states

Male palp

1. FA: absent/femora smooth, 0; present, 1. Modified from character 1 in Benjamin (2010).
   FA is defined here as any projection on the surface of femur. It is present in *Asemonea*, *Pandisu*s, and *Goleba* (Wanless 1980a: figs 4e, 18c). In *Onomastus*, femora are smooth and unmodified, lacking any furrows or apophyses (Benjamin 2010: fig. 26b; Wanless 1980b: figs 1c, 3b).
2. Position of FA: retrolateral/distal, 0; ventral/median, 1. Modified from character 2 in Benjamin (2010).
   Refers to the position of the FA mentioned above. FA is more towards the ventral surface of the centre of the femur in *Goleba* (Wanless 1980a: figs 22c, d, 24b), whereas it is in a distal retrolateral position in *Asemonea* and *Pandisus* (Wanless 1980a: figs 4e, 18c). Wanless (1980a) described state 1 found in *Goleba* as 'ventral tubercle on the palpal femur'.
3. Femoral groove: absent, 0; present, 1. Modified from character 3 in Benjamin (2010).
   Femoral groove is defined as a cavity on the surface of the femur. It does not project outwards as in the FA. The femoral groove is only present in *Asemonea* (Wanless 1980a: figs 10e, 13c). In *Onomastus* femora are smooth and unmodified, lacking any furrows (Benjamin, 2010: fig. 26b).

4. PA: absent, 0; present, 1. Modified from character 4 in Benjamin (2010).
   Present in all *Onomastus* and *Pandisus* (Benjamin 2010: figs 9b, 10a, 14f, 17a; Wanless 1980a; Wanless 1980b). *Onomastus* species lack RTA; instead of RTA, patella of the male palp is armed with an apophysis at the distal end that probably functions as a replacement of RTA. PA is also present in *Pandisus*, as illustrated for *P. scalaris* by Wanless (1980a: fig. 3). One would consider the PA to be homologous in both genera. However, it appears to be otherwise.
5. PA shape: tapering, 0; blunt, 1. Modified from character 5 in Benjamin (2010).
   PA is rather tapering with a smooth rounded tip in all *Onomastus*, except *O. complexipalpis* and *O. kanoi*. In *O. complexipalpis* and *O. kanoi*, the PA broadens towards the end (Benjamin 2010: figs 2a–c, 7f; Ono 1995: figs 19–20).
6. Relative size of patella: patella = tibia, 0; patella > tibia, 1. Modified from character 6 in Benjamin (2010).
   The relatively elongated patella is unique to the two Indian *Onomastus*, *O. patellaris*, *O. indra* (see Benjamin 2010: figs 4a, b, 17a) and South-east Asian *Onomastus kanoi* (see Ono 1995). Hence, the origin of the specific name '*patellaris*', which was the first *Onomastus* species to be described from India.
7. Tibia with ventral or dorsal apophysis: absent, 0; ventral, 1; dorsal, 2.
   The distal ends of the tibia of male palps of all *Onomastus* are smooth without any apophysis. *Pandisus sarae* and *Asemonea tenuipes* have distal, dorsal tibial apophysis (Wanless 1980a: figs 4d, e, 18c, e) and *Goleba puella* with ventral tibial apophysis at the distal end (Wanless 1980a: figs 18c-e). Others lack ventral or dorsal tibial apophysis.
8. RTA: present, 0; absent, 1.
   A RTA is absent in *Onomastus*. All outgroup taxa have retrolateral apophysis in palpal tibia. As a member of the RTA clade, one would expect to see a RTA in all *Onomastus*. However, this is not the case and it is presumed lost in all species (Wanless 1980b).
9. Shape of RTA: tapered, 0; blunt, 1; bifurcated, 2.
   This character defines the RTA in the outgroup taxa. The RTA of *Hispo cingulata* is comparably large and ends apically with a partially bifurcated tip (Wanless 1981: fig. 11c). In *Lyssomanes viridis*, the RTA is very short and pointed distally and hardly noticeable (Edwards 2015: figs 40 a–b; Galiano 1980). In all other outgroup taxa the RTA is comparably larger and ends with a blunt tip.
10. Conductor: absent, 0; present, 1. Modified from character 8 in Benjamin (2010).
    A very complex conductor is present in all known *Onomastus* species and is species-specific in size and shape (Figs 3C, D, 6B, C, D, 9B, D, E; Benjamin 2010: figs 2f, g, 5a, b, 9a; Wanless 1980b). *Hispo cingulata* has a slender conductor originating at the base of the embolus (Wanless 1981: figs 11 a, b).
11. Type of conductor: hyaline, 0; sclerotized, 1. Modified from character 9 in Benjamin (2010).
    A hyaline conductor also termed 'membraneous secondary conductor' by Wanless (1980a: figs 2g, h), is a conductor that is translucent and very thin. A hyaline conductor is present in *Chinoscopus* Simon, 1901 and *Lyssomanes* (Galiano 1962, 1980; Wanless 1980a: figs 2g, h). The presence of a hyaline conductor might turn out to be a synapomorphy that unites *Chinoscopus* and *Lyssomanes*, two exclusively New World genera. Based on illustrations of Wanless (1981), we assumed that *H. cingulata* has a sclerotized conductor; we were unable to examine male specimen due to lack of materials.
12. Shape of conductor: slender, 0; stout, 1; broad, 2; disk, 3; fan, 4. Modified from character 10 in Benjamin (2010).
    Shape of conductor in *Onomastus* varies from a stout apophysis to a large disk-shaped structure. Scored as stout for *Onomastus* of Sri Lanka (Figs 2A, 3A, D, 6D; Benjamin 2010: figs 11d, e, 19b, e) and India (Benjamin 2010: figs 4a, 17a), as broad for two species of the South-East Asian clade *O. nigrimaculatus* and *O. kaharian* and as disk-shaped for *O. complexipalpis* and *O. kanoi* (Benjamin 2010: figs 2b, 3a, 7c-d). All outgroup taxa except for *L. viridis* and *H. cingulata* lack a conductor.
13. Number of hooks on the tip of C: smooth, no hooks, 0; one, 1; two, 2. Modified from character 11 in Benjamin (2010).
    The conductor tip of *O. indra*, *O. kanoi*, and *O. patellaris* is furnished with a single hook (Benjamin 2010: figs 4a, 7a, e, 17a). The rest have a bifurcated tip ending with two pointed hooks (Figs 6B, E; Benjamin 2010: figs 11a–c, 25b, e, h, 28 a, b, e).
14. MA: absent, 0; present, 1. Modified from character 12 in Benjamin (2010).

All known species of *Onomastus* have a sclerotized MA. It is species-specific in shape (Figs 3A, D, E, 6B, D, 9B, D, E; Benjamin 2010: figs 7a, e, 11d, 14d, e, 17a, 20d, e, 25g, h; Wanless 1980b). In some species, it is branched. MA is present in *Hispo* (Wanless 1981: figs 11a, b) and *Lyssomanes* (Galiano 1980a) as well. However, it is absent in *Chinoscopus* (Wanless 1980a: fig. 2h).

15. MA distal end: smooth/tapering, 0; partially bifurcated, 1; strongly bifurcated, 2; with hook, 3; chisel-shaped, 4; scoop-like, 5. Modified from character 13 in Benjamin (2010).
Prolateral and retrolateral arms have been named in relation to their respective position in the palp. The MA in *O. rattotensis* and *O. corbetensis* is strongly bifurcated and diverge into prolateral and retrolateral branches (scored 2; Figs 6B, D; Benjamin 2010: figs 27a, 28a, b). In *O. nigricauda*, *O. kanoi* and *O. complexipalpis*, the MA is chisel-shaped (Benjamin 2010: figs 2b, f, 7a, e, 11b, d, 12a). In *O. jamestaylori* the MA is partially bifurcated and the arms are of equal length (Figs 2A, 3A, D, E). In all other *Onomastus,* the MA is smooth and tapering (Figs 9B, D, E; Benjamin 2010: figs 6b, d, 14d, e, 17a, 20a, d, 25g, h). *Hispo cingulata* has a small and slender MA ending in a distal hook (Wanless 1981: figs 11a, b) whereas *L. viridis* has a tapered MA to a point (scored 0; Edwards 2015: figs 40 a–b).
16. MA with apical hump: absent, 0; present, 1.
The two species *O. pethiyagodai* and *O. quinquenotatus* possess a prominent apical hump at the distal end of MA (Benjamin 2010: figs 19a, c, d, e, f, 20a, d, e, 25a, b, d, e, g, h).
17. Surface of prolateral branch of MA: smooth, 0; with ridges giving a pleated appearance, 1.
In *O. rattotensis* and *O. corbetensis* the prolateral arm of the MA is pleated (Figs 6B, D; Benjamin 2010: figs 27a, 28a, b, c). *Onomastus nigricauda*, *O. complexipalpis*, *O. kanoi* and *O. jamestaylori* with partially bifurcated prolateral arm without pleats (Figs 2A, 3A, D, E; Benjamin 2010: figs 2b, f, 7a, e, 11b, d, 12a). All other applicable species are scored 0.
18. MA with retrolateral branch: absent, 0; present, 1.
Onomastus nigricauda, *O. complexipalpis*, *O. kanoi* and *O. jamestaylori* have weakly developed retrolateral arm (Figs 2A, 3A, D, E; Benjamin 2010: figs 2b, f, 7a, e, 11b, d, 12a) and were scored as 1. *Onomastus rattotensis* and *O. corbetensis* with well-developed curved retrolateral arm were also scored as 1 (Figs 5A, 6B, D; Benjamin 2010: figs 27a, 28a, b, f). All other applicable species are scored 0.
19. Distal end of the retrolateral arm: smooth, 0; serrated, 1; with small indentation, 2; hook, 3.
Retrolateral arm of *O. nigricauda*, *O. complexipalpis* and *O. kanoi* has a smooth tip (Benjamin 2010: figs 2b, f, 7a, e, 11b, d, 12a). The tip of the retrolateral arm of *O. rattotensis* has a hook, *O. corbetensis* has a small indentation and in *O. jamestaylori* the tip of the retrolateral arm is serrated (Figs 2A, 3A, D, E, 5A, 6B, D; Benjamin 2010: figs 27a, 28a, b, f).
20. MAP: absent, 0; present, 1. Modified from character 14 in Benjamin (2010).
The MA has a mesal branch that supports the conductor embolus complex. It is present in all known species from Sri Lanka and India (Benjamin 2010: figs 4a, 11d, 19e, 27a).
21. Origin of embolus: dorsal, 0; basal, 1; median, 2; apical, 3. Modified from character 15 in Benjamin (2010).
The embolus originates from the dorsal parts of tegulum between the tegulum and cymbium in all *Onomastus* species (Benjamin 2010: figs 9a, 15a, b; Wanless 1980b). The origin of the embolus is visible when male palps are cleared with methyl salicylate. It is also clearly visible in the expanded palp (Benjamin 2010: fig. 9a). This character is diagnostic for *Onomastus*. In outgroup taxa, the embolus originates ventrally from different locations of the tegulum.
22. Length of embolus: short, 0; equal or shorter than the circumferences of the tegulum, 1; longer than the circumferences of the tegulum, 2.
Embolus length is assessed based on the number of rotations around the tegulum. *Onomastus complexipalpis* and *O. kanoi* are scored as 2, as the embolus is longer than one rotation around the tegulum (Ono 1995: figs 19, 20). All outgroup taxa possess a moderately long embolus (scored 1), except for *L. viridis*, which has a very short, probably fixed embolus, that originates from apical region of tegulum (scored 0; Galiano1980; Edwards 2015: figs 40 a–b). This character might turn out to be highly homoplasious in broader cladistic studies.
23. Shape of embolus: stout & hook-shaped, 0; filiform, 1; proximally stout & distally filiform, 2; slender, 3; sturdy, 4.
In ingroup taxa, *O. complexipalpis* and *O. kanoi* have thread-like embolus compared to their congeners. Outgroup taxa have different shapes of embolus as mentioned in states.

24. TA1: absent, 0; present, 1. Modified from character 16 in Benjamin (2010).
Male palps of *Onomastus* possess three different tegular structures. Each originates from different positions of the tegulum. They are named as TA1, TA2 and TA3 in Benjamin (2010). TA1 ('y' in Wanless 1980b); 'subtegular apophysis' in Zhang & Li (2005) is unique to *Onomastus* (Figs 3A, 5A, 6A, B, 8A, 9B, E; Benjamin 2010: figs 4a, 10a, 14f, 17a, 25b, e, 28a). TA1, a finger-like projection, is not known to occur in any other Salticidae (Wanless 1980a, b). This character is diagnostic for *Onomastus*.
25. TA2: absent, 0; present, 1. Modified from character 17 in Benjamin (2010).
In addition to TA1, the male palps of Indian *Onomastus* carry a second tegular apophysis termed TA2 ('x' in Wanless 1980b). It originates from the prolateral margin of the male palp, distally to the TA1 (Benjamin 2010: figs 4a, 17a). The presence of TA2 is unique to the two Indian *Onomastus*, *O. patellaris* and *O. indra* (Benjamin 2010: figs 4a, 17a).
26. TA3: absent, 0; present, 1. Modified from character 18 in Benjamin (2010).
TA3 is comparably very shorter than TA1 and TA2 and is situated distally to TA1 and TA2 on the ventral/distal surface of the tegulum (Benjamin 2010: figs 25h, 28d). TA3 is present in all known species of *Onomastus* from Sri Lanka and India (Figs 3A, 5A, 6A, B, 8A, 9B, E; Benjamin 2010: figs 4a, 9b, 19e, 25e, h, 27a, 28d).
27. Shape of tegulum: irregular, 0; elongated, 1; ovoid, 2; bulbous, 3.
Onomastus has a characteristic irregularly shaped tegulum with sinuous ducts (Figs 3A, 5A, 6B, 8A, 9B, E; Benjamin 2010: figs 4a, 9b, 19e, 25e, 27a). Tegulum of *H. cingulata* is pleated and folded distally (Wanless 1981: figs 11a, b), whereas *G. puella* has an elongated tegulum with a flange on the apical-dorsal surface to support the tip of the embolus (Wanless 1980a: figs 22c, e).

Female genitalia

28. Female copulatory ducts: absent, 0; present, 1. Modified from character 19 in Benjamin (2010).
Copulatory ducts are absent in *Onomastus* (Wanless 1980b). Exceptions are *O. kaharian*, *O. complexipalpis*, and *O. simoni*, all the South-East Asia clade (Benjamin 2010: figs 3b, 5d, e). However, the condition in *O. nigrimaculatus* is probably intermediary and is scored as unknown (?). Zhang & Li (2005) stated that there are oval structures directly connected to the anterior wall of the receptacles and these oval structures could be the copulatory ducts. The copulatory ducts of *O. pethiyagodai* are also unknown, because duct-like structure was noticed on the wall of spermathecae and this confusion remains unclear (Benjamin 2010: figs 21b, c). Copulatory ducts are present in all outgroup taxa (Wanless 1980a). The female of *O. kanoi* remains unknown; scored as ?.
29. EF: absent, 0; partially developed, 1; completely developed, 2. Modified from character 20 in Benjamin (2010).
EF, also called 'septum' in Zhang & Li (2005) and Prószyński & Deeleman-Reinhold (2013), is absent in most *Onomastus*; instead, CO is a simple opening in the cuticle (Wanless 1980b). The exceptions are species of the South-East Asian clade (Benjamin 2010: figs 3b, 5c, e, 16c–e; Zhang & Li 2005: figs 5c–e). In *O. complexipalpis*, EF is a weakly developed anterior median septum (Prószyński & Deeleman-Reinhold 2013: figs 106, 107). EF is also absent in the outgroup taxa except for *Asemonea tenuipes* with well-developed median septum (Wanless 1980a).
30. Epigynal lip: absent, 0; present, 1. Modified from character 21 in Benjamin (2010).
A well-developed epigynal lip, also known as epigynal scape, is a tongue-like structure present only in *G. puella* (Wanless 1980a: figs 23a, b). In *H. cingulata*, epigynal lip is comparably very small and a lobe-like structure; scored 1.
31. Shape of spermathecae: round, 0; oval, 1; inverted pear-shaped, 2; irregular, 3; lobed, 4; dumb-bell, 5; kidney, 6.
Prószyński & Deeleman-Reinhold (2013) stated that compact round body with a few internal coiled chambers could be considered as spermathecae in *O. complexipalpis*, but this confusion remains unclear. Phylogenetically unrelated species *Labullinyphia tersa* of family Linyphiidae shows close similarities in epigynal structures of *O. complexipalpis* (see Benjamin & Hormiga 2009: figs 4a, b).

Somatic morphology

32. Number of eye rows: three, 0; four, 1. Modified from character 22 in Benjamin (2010).

Three in *H. cingulata* (Wanless 1981). Four in all other taxa in our matrix (Galiano 1962, 1980; Wanless 1980a, b).

33. Relative size of PME: PME < PLE, 0; PME = PLE, 1. Character 23 in Benjamin (2010).
PME = PLE in *Asemonea* and *Goleba*. PME < PLE in the rest. Outgroups are scored based on Wanless (1980a). This character might be informative in much broader cladistic studies as well.
34. Relative distance between PME–PME vs. ALE–ALE: PME–PME subequal or longer than ALE–ALE, 0; PME–PME < ALE–ALE, 1. Character 24 in Benjamin (2010).
This character was proposed to define a grouping of genera consisting of *Asemonea*, *Goleba*, *Macopaeus*, and *Pandisus* by Wanless (1980a), which he termed group III. Group III was considered by him to be related to group II, which consisted of the genera *Lyssomanes* and *Chinoscopus*. However, *Onomastus* was considered not closely allied to either of them and was, thus, placed in group I (Wanless 1980a). This character might be informative in much broader cladistic studies as well.
35. Prosoma coloration: red/brown, 0; light green, 1. Character 26 in Benjamin (2010).
Lyssomaninae are translucent green in colour (Wanless 1980a; Maddison & Needham 2006). However, available information in the literature on prosoma coloration is rather scanty. All *Onomastus* are clearly green (Benjamin 2010: figs 8a–d, 18a–f) and so are *A. tenuipes* and *L. viridis* (pers. observ.). The remaining taxa are scored based on the descriptions by Wanless (1980a, 1981).

Results and discussion

Heuristic searches resulted in 8 most parsimonious trees under equal weights (best score 70) and five trees under implied weights (L=72, CI= 0.86, RI= 0.86). These five trees differ only in the placement of the South-East Asian clade. The strict consensus of these five trees is given in Fig. 10 (L= 74, CI = 0.81, RI = 0.81). One of the five most parsimonious trees mentioned above is considered as the preferred hypothesis for *Onomastus* phylogenetic relationships (Fig. 11). The strict consensus of the 8 trees recovered under equal weights is given in Fig. 12 (L=82, CI=0.73, RI=0.70).

As in Benjamin (2010), irrespective of the used phylogenetic methodology, all searches recovered a well-supported, monophyletic *Onomastus*. The monophyly of *Onomastus* is supported by the following putative synapomorphies: presence of PA, absence of RTA, hooks on the tip of conductor and presence of TA1.

Within the South-East Asian clade, *O. complexipalpis* and *O. kanoi* are sister species (Figs 10–12), supported by the presence of a blunted PA and a very long and filiform embolus. A clade of *O. nigrimaculatus* and *O. kaharian* is recovered in some searches and expectedly poorly supported. Characters that support this relationship include the presence of a broad conductor and a well-developed epigynal fold. However, a fully developed EF (character 29-2) is present in *Asemonea tenuipes* as well.

On the three new species, *O. corbetensis* and *O. rattotensis* are sister species (Figs 10–12). Genital morphology of both species provides robust support for this placement. *Onomastus jamestaylori* is in a group with *O. nigricauda* and *O. corbetensis* + *O. rattotensis*. This clade is supported by the presence of MA with a retrolateral branch (18-1). *Onomastus maskeliya* is recovered as sister to *O. quinquenotatus* + *O. pethiyagodai*, supported by the irregular shaped spermathecae (31-2).

Searching for the closest relative of *Onomastus*, monophyly of Onomastinae and relationships with Asemoneinae and Lyssomaninae (*sensu* Maddison 2015) is beyond the scope of this paper. However, we would like to point out that, as in Benjamin (2010), this study corroborates *Lyssomanes viridis* as sister to the *Onomastus* clade. This relationship is well supported based on morphology (Figs 10, 12). *Pandisus* clade is supported by five unambiguous synapomorphies (1-1, 7-2, 10-0, 14-0, 34-1). Further, *Asemonea tenuipes* + *Goleba puella* are sister to *Pandisus sarae*, supported by following unambiguous synapomorphies 23-2 (shape of embolus) and 33-0 (relative size of PME).

TABLE 1. Phylogenetic data matrix scored for thirteen *Onomastus* species and five outgroup taxa. The first state is ''0'', followed by ''1'', etc., ''?'' denotes missing data, ''–'' is inapplicable.

Taxon	Characters																																		
										1											2									3					
	1	2	3	4	5	6	7	8	9	0	1	2	3	4	5	6	7	8	9	0	1	2	3	4	5	6	7	8	9	0	1	2	3	4	5
Hispo cingulata	0	-	-	0	-	0	0	0	1	1	1	4	0	1	3	0	0	-	-	0	2	1	4	0	0	0	2	1	0	1	5	0	1	0	0
Pandisus sarae	1	0	0	1	0	0	2	0	0	0	-	-	-	0	-	0	-	-	-	-	1	1	3	0	0	0	3	1	0	0	1	1	1	1	1
Asemonea tenuipes	1	0	1	0	-	0	2	0	0	0	-	-	-	0	-	0	-	-	-	-	1	1	2	0	0	0	2	1	2	0	6	1	0	1	1
Goleba puella	1	1	0	0	-	0	1	0	0	0	-	-	-	0	-	0	-	-	-	-	1	1	2	0	0	0	1	1	0	1	4	1	0	1	1
Lyssomanes viridis	0	-	-	0	-	0	0	0	0	1	0	3	0	1	0	0	0	0	-	0	3	0	0	0	0	0	0	1	0	0	1	1	1	0	1
O. nigrimaculatus	0	-	0	1	0	0	0	1	-	1	1	1	2	1	4	0	0	0	-	0	0	1	3	1	0	?	0	?	2	0	1	1	1	0	1
O. nigricauda	0	-	0	1	0	0	0	1	-	1	1	0	2	1	1	0	0	1	0	1	0	1	3	1	0	1	0	0	0	0	3	1	1	0	1
O. patellaris	0	-	0	1	0	1	0	1	-	1	1	0	1	1	0	0	0	0	-	1	0	1	3	1	1	1	0	0	0	0	1	1	1	0	1
O. quinquenotatus	0	-	0	1	0	0	0	1	-	1	1	0	2	1	0	1	0	0	-	1	0	1	3	1	0	1	0	0	0	0	2	1	1	0	1
O. indra	0	-	0	1	0	1	0	1	-	1	1	0	1	1	0	0	0	0	-	1	0	1	3	1	1	1	0	0	0	0	3	1	1	0	1
O. pethiyagodai	0	-	0	1	0	0	0	1	-	1	1	0	2	1	0	1	0	0	-	1	0	1	3	1	0	1	0	?	0	0	2	1	1	0	1
O. rattotensis	0	-	0	1	0	0	0	1	-	1	1	0	2	1	2	0	1	1	3	1	0	1	3	1	0	1	0	0	0	0	0	1	1	0	1
O. complexipalpis	0	-	0	1	1	0	0	1	-	1	1	2	2	1	1	0	0	1	0	0	0	2	1	1	0	0	0	1	1	0	3	1	1	0	1
O. kanoi	0	-	0	1	1	1	0	1	-	1	1	2	1	1	1	0	0	1	0	0	0	2	1	1	0	0	0	?	?	?	?	1	1	0	1
O. kaharian	0	-	0	1	0	0	0	1	-	1	1	1	2	1	5	0	0	0	-	0	0	1	3	1	0	0	0	1	2	0	0	1	1	0	1
O. corbetensis	0	-	0	1	0	0	0	1	-	1	1	0	2	1	2	0	1	1	2	1	0	1	3	1	0	1	0	0	0	0	0	1	1	0	1
O. maskeliya	0	-	0	1	0	0	0	1	-	1	1	0	2	1	0	0	0	0	-	1	0	1	3	1	0	1	0	0	0	0	2	1	1	0	1
O. jamestaylori	0	-	0	1	0	0	0	1	-	1	1	0	2	1	1	0	0	1	1	1	0	1	3	1	0	1	0	0	0	0	1	1	1	0	1

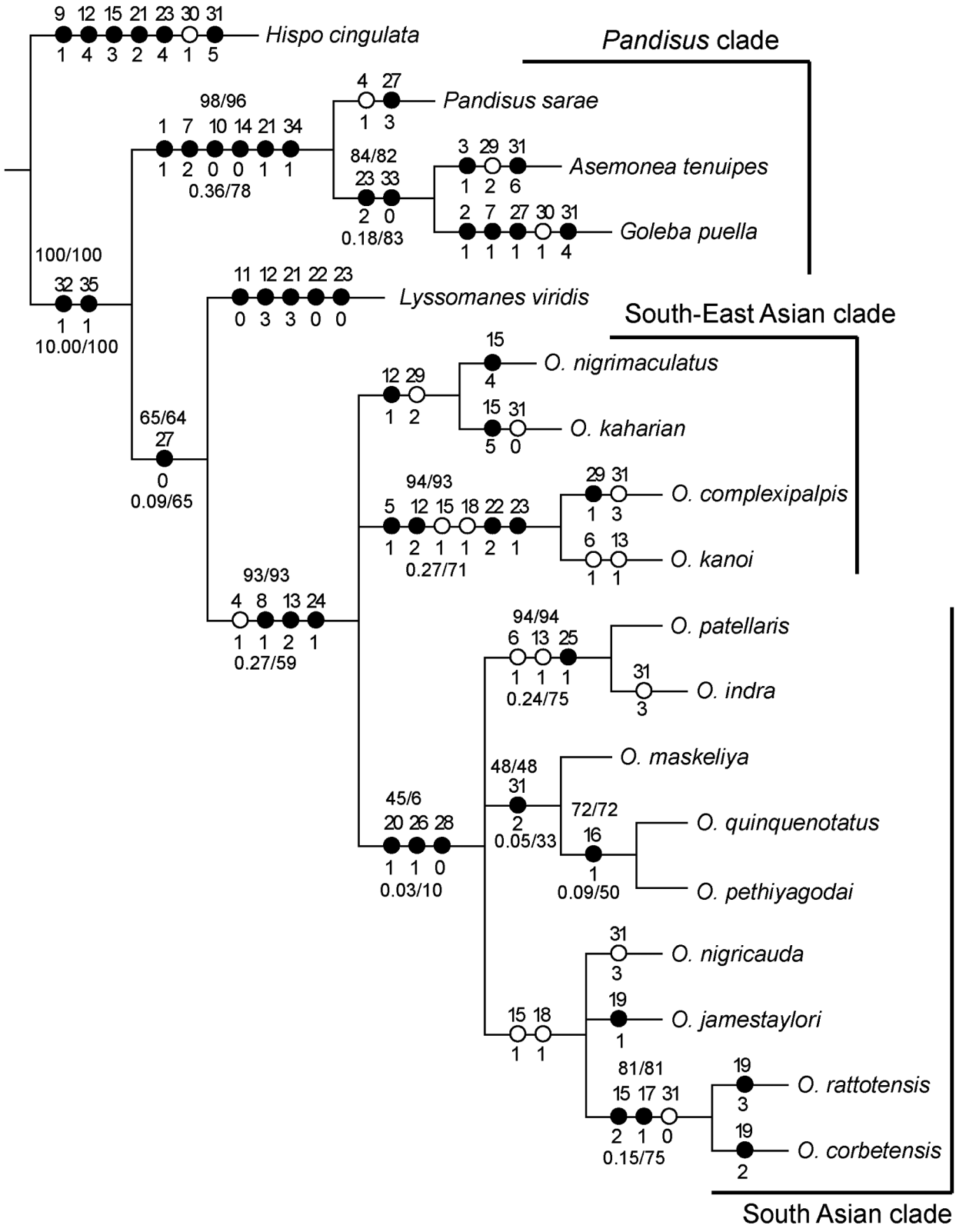

FIGURE 10. Phylogenetic placement of the jumping spider genus *Onomastus* Simon, 1900 obtained by the analysis of 35 morphological characters under implied weights. Strict consensus (L= 74 steps, CI= 0.81, RI= 0.81) of five most parsimonious trees. Unambiguous character state changes are mapped using Farris optimization. Characters are denoted by the numbers above the circles and character state changes by numbers below the circles. The values at the top of each node represent sympatric resampling frequencies/sympatric resampling frequency differences, while the values at the bottom of nodes represent Bremer support/relative Bremer support.

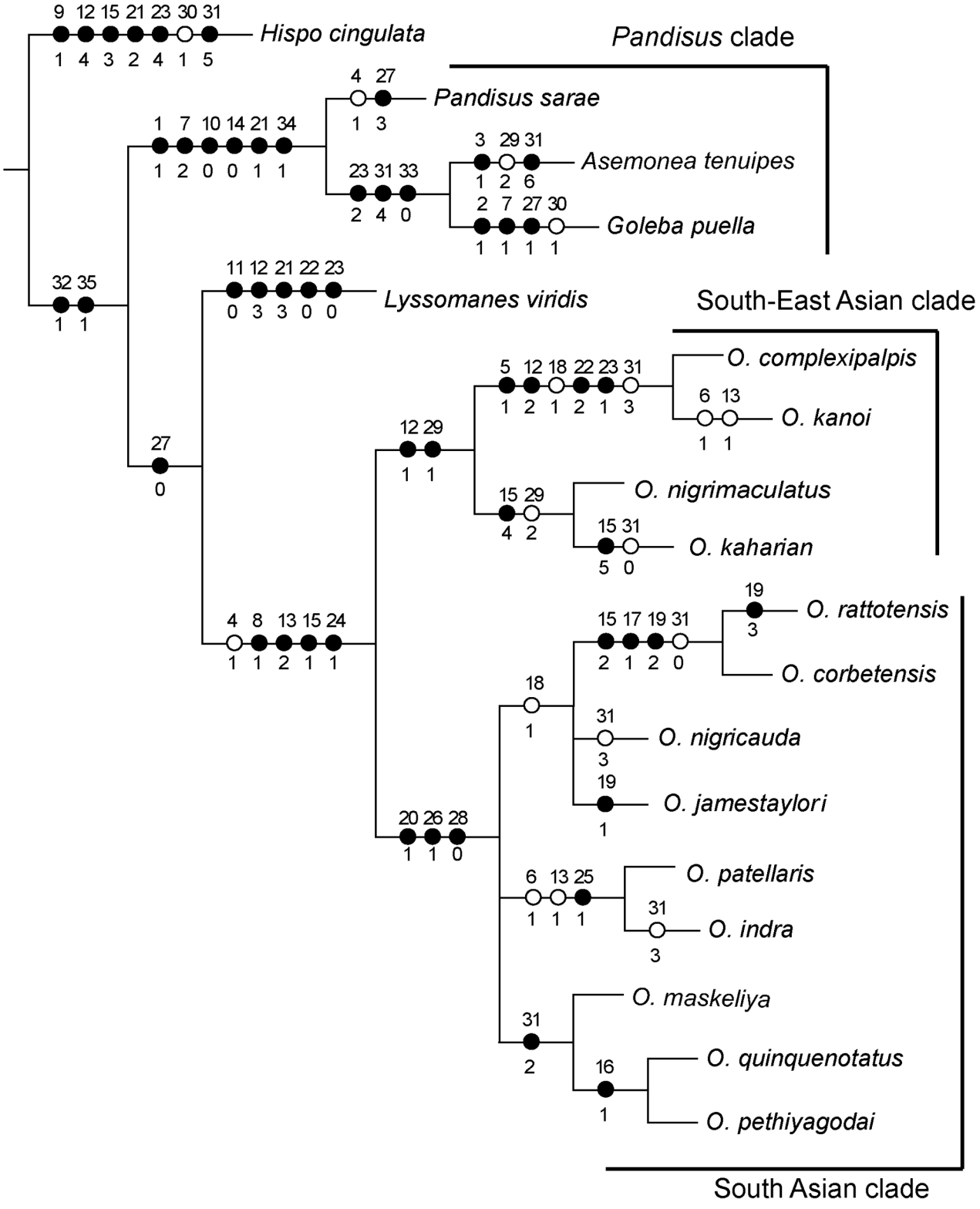

FIGURE 11. Phylogenetic placement of the jumping spider genus *Onomastus* Simon, 1900. One of the five most parsimonious tree obtained under implied weights (L= 70 steps, CI= 0.85, RI= 0.86). Unambiguous character state changes are mapped using Farris optimization. Characters are denoted by the numbers above the circles and character state changes by numbers below the circles.

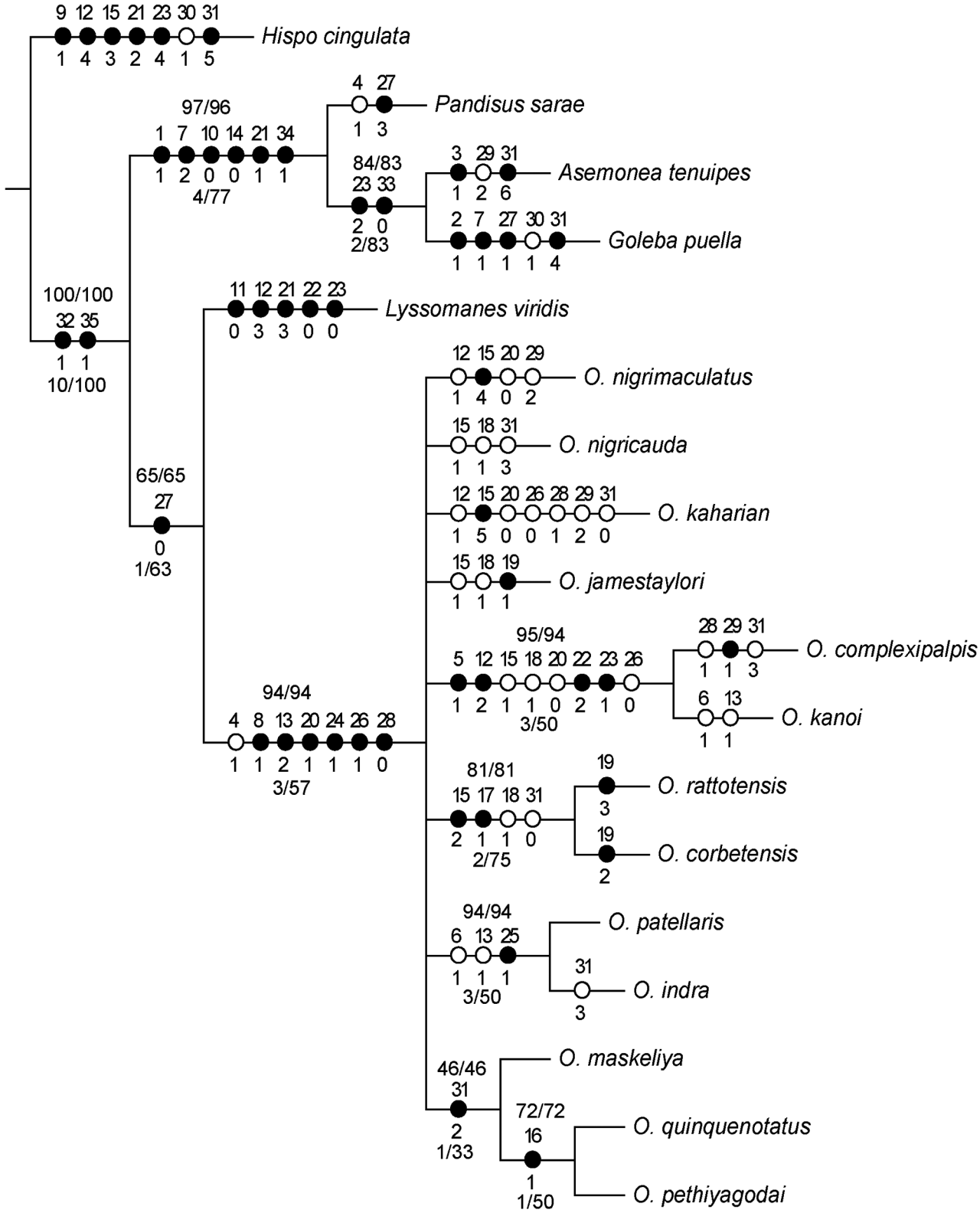

FIGURE 12. Phylogenetic placement of the jumping spider genus *Onomastus* Simon, 1900 obtained by the analysis of 35 morphological characters under equal weights. Strict consensus (L= 82 steps, CI= 0.73, RI= 0.70) of the eight most parsimonious trees. Unambiguous character state changes are mapped using Farris optimization. Characters are denoted by the numbers above the circles and character state changes by numbers below the circles. The values at the top of each node represent sympatric resampling frequencies/sympatric resampling frequency differences, while the values at the bottom of nodes represent Bremer support/relative Bremer support.

Conservation status

All three new species are known from relatively few individuals and are restricted to high altitude cloud forest (1300–1800m) in the Central Province of Sri Lanka. The known localities are within protected areas. However, they are increasingly threatened due to woodcutting of old trees for timber, fire wood collection, cultivation of vegetables/cardamom and simple vandalism. Climate change may pose a further threat to these three cloud forest endemics. Assessment against the IUCN criteria (IUCN 2001) results in a status of vulnerable 'VU D1'. This assessment is based on an estimated population of less than 1000 adult spiders.

Acknowledgments

This study was funded by the NIFS with additional funding coming from a fellowship from the Alexander von Humboldt Foundation to SPB. Authors are indebted to G.B. Edwards for information on the morphology of *L. viridis*. Authors are grateful to S. Batuwita, P.M.H. Sandamali and N. Athukorala, who collected and made available many specimens used in this study. The SEMs were taken at the ZFMK with assistance from Karin Ulmen; her assistance is gratefully acknowledged. DWLC and DFC of Sri Lanka facilitated fieldwork; their assistance is very gratefully acknowledged. We thank Indunil Clayton, Gustavo Ruiz and two anonymous reviewers for helpful comments.

References

Benjamin, S.P. (2004) Taxonomic revision and a phylogenetic hypothesis for the jumping spider subfamily Ballinae (Araneae, Salticidae). *Zoological Journal of the Linnean Society*, 142, 1–82.
https://doi.org/10.1111/j.1096-3642.2004.00123.x

Benjamin, S.P. (2006) The male of *Marengo nitida* with the description of *M. rattotensis* new species from Sri Lanka (Araneae: Salticidae). *Zootaxa*, 1326, 25–36.

Benjamin, S.P. (2010) Revision and cladistic analysis of the jumping spider genus *Onomastus* (Araneae: Salticidae). *Zoological Journal of the Linnean Society*, 159, 711–745.
https://doi.org/10.1111/j.1096-3642.2009.00580.x

Benjamin, S.P. (2011) *Phylogenetics and comparative morphology of crab spiders (Araneae: Dionycha, Thomisidae)*. *Zootaxa*, 3080, 1–108.

Benjamin, S.P. & Hormiga, G. (2009) Phylogenetic placement of the enigmatic genus *Labullinyphia* van Helsdingen, 1985, with redescription of *Labullinyphia tersa* (Simon, 1894) from Sri Lanka (Araneae: Linyphiidae). *Contributions to Natural History*, 12, 161–181.

Bremer, K. (1988) The limits of amino acid sequence data in angiosperm phylogenetic reconstruction. *Evolution*, 42. 795–803.
https://doi.org/10.2307/2408870

Bremer, K. (1994) Branch support and tree stability. *Cladistics*, 10, 295–304.
https://doi.org/10.1111/j.1096-0031.1994.tb00179.x

Dingerkus, G. & Uhler, L.D. (1977) Enzyme clearing of alcian blue stained whole small vertebrates for demonstration of cartilage. *Stain Technology*, 52, 229–232.
https://doi.org/10.3109/10520297709116780

Edwards, G.B. (2015) Freyinae, a major new subfamily of Neotropical jumping spiders (Araneae: Salticidae). *Zootaxa*, 4036, 1–87.
https://doi.org/10.11646/zootaxa.4036.1.1

Farris, J.S. (1970) Methods for computing Wagner trees. *Systematic Zoology*, 19, 83–92.
https://doi.org/10.2307/2412028

Fitch, W.M. (1971) Toward defining the course of evolution: minimum change for a specific tree topology. *Systematic Biology*, 20, 406–416.
https://doi.org/10.1093/sysbio/20.4.406

Galiano, M.E. (1962) Redescripciones de especies del gnero *Lyssomanes* Hentz, 1845, basadas en los ejenplares tpicos. Descripcin de una especie nueva (Araneae: Salticidae). *Acta zoologica Lilloana*, 18, 45–97.

Galiano, M.E. (1980) Revisin del gnero *Lyssomanes* Hentz, 1845 (Araneae: Salticidae). *Opera Lilloana*, 30, 1–104.

Goloboff, P.A., Farris, J.S., Källersj, M., Oxelman, B., Ramírez, M.J. & Szumik, C.A. (2003) Improvements to resampling measures of group support. *Cladistics*, 19, 324–332.
https://doi.org/10.1111/j.1096-0031.2003.tb00376.x

Goloboff, P.A., Farris, J.S. & Nixon, K. (2008) TNT: a free program for phylogenetic analysis. *Cladistics*, 24, 774–786. https://doi.org/10.1111/j.1096-0031.2008.00217.x

Maddison, W.P. (2015) A phylogenetic classification of jumping spiders (Araneae: Salticidae). *Journal of Arachnology*, 43, 231–292. https://doi.org/10.1636/arac-43-03-231-292

Maddison, W.P. & Maddison, D.R. (2009) Mesquite: a modular system for evolutionary analysis. *In:* Version 2.72 http://mesquiteproject.org

Maddison, W.P. & Needham, K.M. (2006) Lapsiines and hisponines as phylogenetically basal salticid spiders (Araneae: Salticidae). *Zootaxa*, 1255, 37–55.

Nixon, K.C. (2002) *WinClada*. Published by the Author, Ithaca, New York.

Ono, H. (1995) Four East Asian spiders of the families Eresidae, Araneidae, Thomisidae and Salticidae (Arachnida, Araneae). *Bulletin of the national science museum, Series A (Zoology)*, 21, 157–156.

Prószyski, J. & Deeleman-Reinhold, C.L. (2013) Description of some Salticidae (Aranei) from the Malay Archipelago. III. Salticidae of Borneo, with comments on adjacent territories. *Arthropoda Selecta,* 22, 113–144.

Simon, E. (1900) tudes arachnologiques. 30e Mémoire. XLVII. Descriptions d'espèces nouvelles de la famille des Attidae. *Annales de la Société entomologique de France*, 69, 27–61.

Wanless, F.R. (1980a) A revision of the spider genera *Asemonea* and *Pandisus* (Araneae: Salticidae). *Bulletin of the British Museum (Natural History) Zoology*, 39, 213–257.

Wanless, F.R. (1980b) A revision of the spider genus *Onomastus* (Araneae: Salticidae). *Bulletin of the British Museum (Natural History) Zoology*, 39, 179–188.

Wanless, F.R. (1981) A revision of the spider genus *Hispo* (Araneae: Salticidae). *Bulletin of the British Museum (Natural History) Zoology* 41, 179–198.

World Spider Catalog (2016) *World Spider Catalog*. Natural History Museum Bern. [version 16.5] Available from: http://wsc.nmbe.ch (accessed 25 April 2016)

Zhang, J.X. & Li, D. (2005) Four new and one newly recorded species of the jumping spiders (Araneae: Salticidae: Lyssomaninae & Spartaeinae) from (sub) tropical China. *Raffles Bulletin of Zoology*, 53, 221–229.